Chapitre 5

Variabilité dans le bassin occidental : la Western Mediterranean Transition (WMT)

Ce chapitre est consacré à l'étude de la Western Mediterranean Transition (WMT), phénomène illustrant la variabilité à long terme dans le bassin méditerranéen occidental.
Dans une première partie, nous nous intéressons à un aspect particulier résultant de la WMT : comme à partir de 2005, les caractéristiques thermohalines de l'eau profonde ouest-méditerranéenne (WMDW) ont changé, il est ainsi plus facile de suivre sa propagation dans le sous-bassin Algéro-Provençal. L'étude présentée dans la section 5.1 utilise les résultats des simulations courtes de MED12-ARPERA pour caractériser l'impact de tourbillons profonds de méso-échelle dans la propagation de la WMDW formée pendant l'hiver 2005.
Dans une deuxième partie, nous analysons ce processus de propagation de la WMDW avec des conditions différentes de forçage, de résolution et de conditions intiales.
Enfin, la WMT est replacée dans la variabilité à long-terme de la convection profonde en Méditerranée nord-occidentale. Les principales conclusions d'une étude avec NEMOMED8 sont tout d'abord présentées, puis nous analysons l'apport du changement de résolution et de conditions initiales (comparaison de la simulation MED12-50ans avec les simulations MED12-ARPERA et la simulation NM8-clim).

5.1 Etude du processus de propagation de la WMDW formée pendant l'hiver 2005

Cette section est consitituée d'un article soumis au Journal of Geophysical Reserach.

Beuvier, J., K. Béranger, C. Lebeaupin Brossier, S. Somot, F. Sevault, Y. Drillet, R. Bourdallé-Badie, N. Ferry, and F. Lyard (soumis), Spreading of the Western Mediterranean Deep Water after winter 2005 : time-scales and deep cyclone transport, *submitted to Journal of Geophysical Research*.

Résumé

Ce travail est consacré à l'étude de la propagation de l'eau ouest-méditerranéenne profonde (*Western Mediterranean Deep Water*, WMDW) formée dans le Golfe du Lion au cours de l'hiver exceptionnel de 2005. Une simulation de la période 1998-2008 a été réalisée avec un

modèle de circulation générale océanique “eddy-resolving” de la mer Méditerranée, forcé par des flux air-mer interannuels et à haute résolution. Cette étude présente tout d'abord une validation des améliorations récentes de la configuration du modèle, face à des observations satellites. Puis, nous évaluons la capacité du modèle à reproduire l'évenement de convection profonde particulièrement intense dans le Golfe du Lion pendant l'hiver 2005. Un volume conséquent d'eau très dense est formé dans la simulation à cette date (taux de formation annuel d'environ 3 Sv). Les caractéristiques thermohalines de la nouvelle WMDW permette de suivre sa propagation en profondeur. Nous identifions plusieurs cyclones profonds comme étant principalement responsables de la propagation rapide de la WMDW vers le Sud dans le bassin occidental de la Méditerranée. En comparant des approches eulériennes et lagrangiennes, nous estimons différents temps de transport de la WMDW par ces tourbillons cycloniques et nous les comparons à ceux déduits des observations. Finalement, nous affirmons que ces cyclones favorisent la propagation des caractéristiques thermohalines de la WMDW vers le canal de Sardaigne et qu'ils diminuent le volume de WMDW qui peut atteindre le détroit de Gibraltar.

Spreading of the Western Mediterranean Deep Water after winter 2005 : time-scales and deep cyclone transport

J. Beuvier, K. Béranger, C. Lebeaupin Brossier, S. Somot, F. Sevault, Y. Drillet, R. Bourdallé-Badie, N. Ferry, F. Lyard.

Abstract

This work is dedicated to the study of the propagation of the Western Mediterranean Deep Water (WMDW) formed in the Gulf of Lions during the exceptional winter 2005. A simulation of the 1998-2008 period has been carried out with an eddy-resolving Ocean General Circulation Model of the Mediterranean Sea, driven by interannual high-resolution air-sea fluxes. This study first presents a validation of the recently improved model configuration against satellite observations. Then, we assess the ability of the model to reproduce the particularly intense deep convection event of winter 2005 in the Gulf of Lions. A huge volume of very dense water is formed in the simulation at that time (annual formation rate of about 3 Sv). The thermohaline characteristics of the new WMDW allow a monitoring of its deep propagation. We identify several deep cyclones as mainly responsible of the fast spreading of the WMDW southwards in the Western Mediterranean. By comparing Eulerian and Lagrangian approaches, we estimate different transport times of the WMDW by these cyclonic eddies and compare them to those deduced from several observations. Finally, we argue that these cyclones favour the propagation of the WMDW thermohaline characteristics towards the Channel of Sardinia and decrease the volume of WMDW which can reach the Strait of Gibraltar.

5.1.1 Introduction

Deep convection occurs in the Mediterranean Sea, in particular in the Gulf of Lions in the Western Mediterranean (GoL in Fig.1). In this particular place, the formation of deep water is mainly triggered by the atmosphere with strong local winds, which lead to a high latent heat loss for the sea (*Schott et al.*, 1996), and by a topographic control (*Madec et al.*, 1996). The formation process was well described by *Marshall and Schott* (1999) in three phases : the preconditionning, the convection and the spreading. The particular circulation through a cyclonic gyre in the Gulf of Lions is enhanced in winter by the winds channeled by the Alps, the Massif Central and the Pyrenees. In the center of this relatively closed gyre, above which strong heat loss occurs, is formed the Western Mediterranean Deep Water (WMDW) in winter. The WMDW plays a major role in the thermohaline circulation of the Mediterranean. This water mass is characterized by a density above 29.10 $kg.m^{-3}$ (*MEDOC Group*, 1970). The convection regularly reaches the sea bottom, which is about 2400 m depth in this area, and occurs around the 42 °N - 5 °E position, as observed for example in 1982 (*THETIS Group*, 1994).
High resolution ocean modelling studies have proved their skill to accurately reproduce the convection process, at basin scale (*Castellari et al.*, 2000; *Artale et al.*, 2002; *Béranger et al.*, 2005; *Fernàndez et al.*, 2005; *Somot et al.*, 2006; *Sannino et al.*, 2009; *Beuvier et al.*, 2010b; *Herrmann et al.*, 2010) or at regional scale in embedded models (*Mantziafou and Lascaratos*, 2004; *Herrmann and Somot*, 2008; *Herrmann et al.*, 2008). In these modelling studies, the atmospheric resolution was proved to be of high importance to allow the simulation of the deep convection without some artificial added forcings. In particular, the wind channeling is one of the main factor that helps the preconditionning phase (*Béranger et al.*, 2010), in producing extreme heat loss (*Herrmann and Somot*, 2008).

During the winter 2005, a drastic convection event occured in the Gulf of Lions (*López-Jurado et al.*, 2005; *Schröder et al.*, 2006; *Canals et al.*, 2006; *Font et al.*, 2007; *Smith et al.*, 2008; *Schroeder et al.*, 2008). Before the event, the previous WMDW has characteristics ranging in 12.75-12.92 °C for potential temperature and in 38.41-38.47 psu for salinity. After the event, the new WMDW potential temperature ranges between 12.87 and 12.90 °C, and, the new WMDW salinity ranges between 38.47 and 38.50 psu. The new WMDW has thus a well marked thermohaline signature, as it is saltier and slightly warmer than the previous one, with a corresponding density range of 29.11-29.13 $kg.m^{-3}$. The formation rate of new WMDW was particularly high compared to other years. *Schroeder et al.* (2008) proposed a value of 2.4 Sv for the two winters 2005 and 2006, while previous estimates are ranged for observations between 0.1 and 1.2 Sv (*Schott et al.*, 1996; *Marshall and Schott*, 1999) and for models between 0.2 and 1.6 Sv (*Castellari et al.*, 2000; *Somot et al.*, 2006; *Béranger et al.*, 2009). An estimate of its time-scale spreading in the Western Mediterranean can be made : the new WMDW thermohaline signature was then detected in the Strait of Gibraltar (SG in Fig. 1) and in the Channel of Sardinia (CS in Fig. 1) by deep observations in 2006. *Schroeder et al.* (2008) argued that it takes less than a year and a half to this new WMDW to spread in the basin, approximately until 3 °W. But because the authors used only bi-annual subsections in the basin, we do not know too much on the processes involved in this very fast spreading of new WMDW. *Testor and Gascard* (2003) and *Testor and Gascard* (2006), using Lagrangian floats during 1994-1995 and 1997-1998, have shown that submesoscale coherent vortices with a typical size of 5-10 km are one of the involved processes. They estimate that such eddies account for as much as 40% of the new WMDW spreading away from the convection area. With a coastal eddy-resolving model of the Gulf of Lions, *Herrmann et al.* (2008) have highlighted that about one third of the deep water advection after the convection event is made southwestwards by very energetic mesoscale structures with a typical size of 25-50 km.
Herrmann et al. (2010) have studied the convection phase of the winter 2005 event and its atmospheric and oceanic preconditionning factors. We here investigate the spreading phase of WMDW in winter 2005 to evaluate how the WMDW can be transported from the Gulf of Lions towards the southern channels and at what time-scale. We want to complete the fragmented view of this spreading given by the observations of *Testor and Gascard* (2003), *Testor and Gascard* (2006) and *Schroeder et al.* (2008), by using the high-resolution 4D view offered by an ocean model. We use an eddy-resolving model, in which we add new parameterizations to improve the model skills (subsection 5.1.2), to study the winter 2005. The formation of WMDW during winter 2005 is first described in the model simulation in subsection 5.1.3. Then the spreading phase is studied using eulerian and lagrangian diagnostics in subsection 5.1.4. Section 5.1.5 is devoted to a conclusion.

5.1.2 Model configuration and simulations

We use the ocean general circulation model NEMO (*Madec and the NEMO Team*, 2008) in a regional configuration of the Mediterranean Sea called MED12 (*Lebeaupin Brossier et al.*, 2011). The model configuration is first described before detailing the differences between three companion simulations used inthis study.

5.1.2.1 Model configuration

The development of MED12 is made in the continuity of the evolution of the French modelling of the Mediterranean Sea, following OPAMED16 (*Béranger et al.*, 2005), OPAMED8 (*Somot et al.*, 2006) and NEMOMED8 (*Beuvier et al.*, 2010b).

Grid and bathymetry

MED12 covers the whole Mediterranean Sea plus a buffer zone including a part of the near Atlantic Ocean (Figure 5.1). It does not cover the Black Sea. The horizontal grid of MED12 comes from the ORCA grid of NEMO at $1/12\,^{\circ}$ horizontal resolution. This corresponds in the Mediterranean area to a grid cell size between 6 and 8 km, from 46 °N to 30 °N.
MED12 has 50 vertical stretched z-levels (from $\Delta z = 1$ m at the surface to $\Delta z = 450$ m at the bottom, with 35 levels in the first 1000 m). The bathymetry comes from the 10^{th} version of the MERCATOR-LEGOS bathymetry at a resolution of 30" × 30", composed of merging between the GEBCO-08 database, the MEDIMAP bathymetry (*Medimap Group*, 2005) and the Ifremer bathymetry of the Gulf of Lions (*Berné et al.*, 2004) . We use a partial cell parameterization, i.e. the bottom layer thickness is varying to fit the real bathymetry.

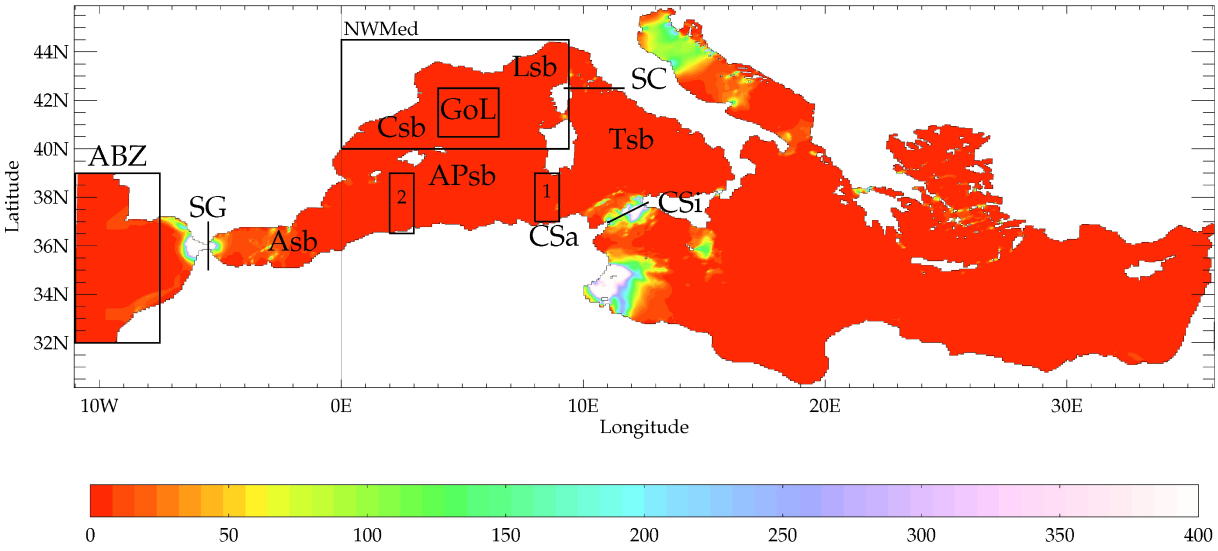

FIG. 5.1 – *The domain of the MED12 model is illustrated by the bottom turbulent kinetic energy background E ($cm^2.s^{-2}$). This field is used in simulations MED12-ARPERA-2 and MED12-ARPERA-3 (maximum value over 10000 $cm^2.s^{-2}$ at the Strait of Gibraltar) while E is equal to a constant of 25 $cm^2.s^{-2}$ in simulation MED12-ARPERA-1. ABZ : Atlantic Buffer Zone, SG : Strait of Gibraltar, CSa : Channel of Sardinia, CSi : Channel of Sicily, SC : Strait of Corsica, GoL : Gulf of Lions, Asb : Alboran subbasin, APsb : Algero-Provencal subbasin, Csb : Catalan subbasin, Lsb : Ligurian subbasin and Tsb : Tyrrhenian subbasin. The Algerian subbasin, when mentionned in the text, corresponds to the southern part of APsb. The rectangle in the north-western Mediterranean is the area where SSH is averaged in section 5.1.3.2. The rectangle in the Gulf of Lions is the area where the density profiles are averaged in section 5.1.3.3. The rectangles 1 and 2 are the boxes of the θ-S diagrams in section 5.1.4.2.*

Physics parameterizations

A time step of 12 minutes is used. The horizontal eddy diffusivity coefficient is set to 60 $m^2.s^{-1}$ for the tracers (temperature, salinity) using a laplacian operator (the diffusion is applied along iso-neutral surfaces for the tracers) and the horizontal viscosity coefficient is set to -1.25×10^{10} $m^4.s^{-2}$ for the dynamics (velocity) using of a biharmonic operator. The TVD (Total Variance Dissipation) scheme is used for the tracer advection and the EEN (Energy and ENstrophy conservative) scheme is used for the momentum advection (*Arakawa and Lamb*, 1981; *Barnier et al.*, 2006). A 1.5 turbulent closure scheme is used for the vertical eddy diffusivity (*Blanke*

and Delecluse, 1993) with an enhancement of the vertical diffusivity coefficient up to $10\,m^2.s^{-1}$ in case of unstable stratification. The solar radiation can penetrate into the ocean surface layers (*Bozec et al.* (2008)). A no-slip lateral boundary condition is used. The bottom friction is quadratic. The evolution of the sea surface is parameterized by a filtered free-surface (*Roullet and Madec*, 2000). The conservation of the model volume is assumed (see subsection 5.1.2.2). The Sea Surface Height (SSH) is a prognostic variable.

Initial conditions in the Mediterranean domain

For the Mediterranean Sea, the initial conditions are provided by the monthly mean potential temperature and salinity 3D fields from the MEDATLAS-II climatology (*MEDAR/MEDATLAS Group*, 2002) corresponding to October. These fields are ponderated by a low pass filtering with a time-window of three years using the MEDATLAS data covering the 1997-1999 period. The simulations then start with initial conditions close to the Mediterranean Sea state of October 1998 and an ocean at rest.

Atlantic boundary conditions

The exchanges with the Atlantic ocean are performed through a buffer zone. From 11 °W to 7.5 °W (ABZ in Figure 1), 3D temperature and salinity of MED12 are relaxed towards the θ-S climatological fields of *Levitus et al.* (2005). The restoring term is weak west of Cadiz and Gibraltar area ($\tau = 90$ days at 7.5 °W) and increases westwards ($\tau = 2$ days at 11 °W).

River runoff and Black Sea inputs

River inputs are introduced as surface freshwater gain at the river mouths. We use the climatological average of the interannual dataset of *Ludwig et al.* (2009) to compute monthly runoff values, split in two parts. First, for the 33 main Mediterranean rivers listed in the RivDis database (*Vörösmarty et al.*, 1996), we directly take the values of the database. Second, the values of the inputs of the other rivers are gathered and averaged in each Mediterranean subbasin (as defined in *Ludwig et al.* (2009)) and put as a coastal runoff in each MED12 coastal grid point of these subbasins. These two types of river inputs contribute for the annual surface freshwater budget of the Mediterranean Sea to $+0.09\,m.yr^{-1}$ for the 33 main rivers and to $+0.05\,m.yr^{-1}$ for the others, $i.e.$ $+0.14\,m.yr^{-1}$ in total, which is in good agreement with the $+0.14\,m.yr^{-1}$ estimate of *Boukthir and Barnier* (2000) and higher than the $+0.10\,m.yr^{-1}$ estimate of *Mariotti et al.* (2002).

The Black Sea is not included in MED12 but is one of the major freshwater sources of the Mediterranean Sea. The exchanges between the Black Sea and the Aegean Sea consist of a two-layer flow across the Marmara Sea and the Dardanelles Strait. We assume that this flow can be approximated by a freshwater flux diluting the salinity of the mouth grid point. Thus, in the model, the Black Sea is considered as a river for the Aegean Sea, as done in *Beuvier et al.* (2010b). We use the climatological average of the interannual dataset of *Stanev and Peneva* (2002) to compute monthly values of the Black Sea net water inflow. The annual average of this input corresponds for the surface freshwater budget of the Mediterranean Sea to $+0.10\,m.yr^{-1}$. So, the total freshwater input from river and Black Sea runoff amounts in our configuration to $+0.24\,m.yr^{-1}$.

Atmospheric forcing

The atmospheric forcing is ARPERA, obtained by performing a dynamical downscaling of ECMWF products above the European-Mediterranean region (*Herrmann and Somot*, 2008). The downscaling method used here is a spectral nudging : it uses the atmospheric model ARPEGE-Climate (*Déqué and Piedelievre* (1995), grid streched over the Mediterranean Sea,

	Standard bilinear bottom friction	Mean tidal effect in the bilinear bottom friction	No SSH condition in the Atlantic	SSH imposed in the Atlantic
MED12-ARPERA-1	x		x	
MED12-ARPERA-2		x	x	
MED12-ARPERA-3		x		x

TAB. 5.1 – *Differences in the boundary conditions between the three companion simulations.*

resolution of 50 km), in which large scales (above 250 km) are spectrally driven by ECMWF fields and small scales (below 250 km) can develop freely. This dataset has a realistic synoptic chronology thanks to ECMWF fields and high-resolution structures thanks to the atmospheric resolution of ARPEGE-Climate. The simulated period lasts from the 1^{st} October 1998 to the 31^{st} December 2008. For the period 1998-2001, the driven fields come from the ERA40 reanalysis (*Simmons and Gibson*, 2000). From 2002 to 2008, fields of the ECMWF analyses are used, their resolution ($0.5\,^\circ \sim 55$ km) being downgraded to the ERA40 resolution ($1.125\,^\circ \sim 125$ km) to insure consistency between the 1998-2001 and 2002-2008 periods. ARPERA follows the real atmospheric chronology and is relevant to model realistically deep convection (*Beuvier et al.*, 2010b; *Herrmann et al.*, 2010). MED12 is forced by ARPERA daily fields of the momentum, freshwater and heat fluxes.
For the surface temperature condition, a relaxation term toward ERA40 Sea Surface Temperature (SST) is applied for the heat flux. This term actually plays the role of a first-order coupling between the SST of the ocean model and the atmospheric heat flux (*Barnier et al.*, 1995), ensuring the consistency between those two terms. The value of the relaxation coefficient is spatially constant and taken equal to $-\,40\,W.m^{-2}.K^{-1}$, following *CLIPPER Project Team* (1999). It is equivalent to a 1.2-day restoring time scale for a surface layer of 1 m thickness.
For the salinity surface boundary condition, no salinity damping is applied. Following *Beuvier et al.* (2010b), we add to the surface freshwater flux (E−P−R) a correction term, spatially constant, with a monthly cycle and equivalent in annual average to -0.0083 mm.d^{-1} (-0.003 m.yr^{-1}), which is neglectable with respect to the total freshwater budget. These monthly values have been computed by averaging the Sea Surface Salinity (SSS) relaxation term through a previous companion simulation with MED12 and the same atmospheric forcing. The surface freshwater budget is thus balanced without altering the spatial and temporal variations of the freshwater flux and so of the SSS. This correction term is added to the water fluxes coming from the atmospheric fields and from the rivers and Black Sea runoff. We note that the total freshwater loss (P+R−E+correction= -0.53 m.yr^{-1} for the 2002-2008 period over the Mediterranean Sea) is in the range of observations and other modelling studies (*Sanchez-Gomez et al.*, 2011).

5.1.2.2 Set of simulations

We performed three companion simulations with the same initial state, atmospheric forcing, Atlantic thermohaline characteristics, river runoff and Black Sea inputs, differing from each other by the choice of two parameterizations : the definition of the bottom friction and the way to keep the model volume constant (see Table 5.1).

The first simulation is called MED12-ARPERA-1. The quadratic bottom friction $\overrightarrow{F}$ parameterization is defined as follows in NEMO :

$$\overrightarrow{F} = C_D \sqrt{U_H^2 + V_H^2 + E}\,\overrightarrow{U_H}$$

with C_D the bottom drag coefficient, U_H and V_H respectively the zonal and meridian velocities of the bottom layer, $\overrightarrow{U_H}$ the horizontal bottom speed vector and E the bottom turbulent kinetic energy background. In this simulation, we use constant values of $C_D = 10^{-3}$ and $E = 25\,\mathrm{cm}^2.\mathrm{s}^{-2}$.

In the second and third simulations, called MED12-ARPERA-2 and MED12-ARPERA-3, E is a 2D field (Figure 5.1) corresponding to the mean tidal energy computed from a tidal model (*Lyard et al.*, 2006). The mean tidal energy is the highest in the Strait of Gibraltar (maximum value over $10000\,\mathrm{cm}^2.\mathrm{s}^{-2}$) and has significant values mainly in the Channel of Sicily, in the Gulf of Gabes and in the northern Adriatic Sea.

As seen in subsection 5.1.2.1, the Mediterranean Sea is known as a basin of net evaporation compensated by the Atlantic inflow. According to the NEMO filtered free sea surface parameterization, only the volume of the first level of the model can change but the total volume of the model is not conserved, which requires thus a parameterization to do so. In MED12-ARPERA-1 and MED12-ARPERA-2 simulations, at each time step, the water volume corresponding to the net evaporation averaged over the Mediterranean Sea (east of Gibraltar) is redistributed in the Atlantic area between 11 °W and 7.5 °W as precipitation, following *Tonani et al.* (2008) and *Beuvier et al.* (2010b).
In MED12-ARPERA-3 simulation, a new parameterization is implemented. The model volume is conserved through a damping of the SSH between 11 °W and 7.5 °W towards a prescribed SSH. We apply a very strong restoring, since its time scale is set to 2 seconds. The reference SSH was built by adding the 2002-2008 mean SSH of MED12-ARPERA-2 with monthly sea level anomalies. For the period 2002-2008 (Figure 5.2a), the anomalies are taken from GLORYS-1 (*Ferry et al.*, 2010), a reanalysis of the global ocean circulation at a $1/4\,^\circ$ horizontal resolution available for this period. For the period 1998-2001, the anomalies are taken from the SSH monthly cycle of MED12-ARPERA-2 with a shift of 5 months in the seasonal cycle to follow the cycle of GLORYS-1 (Figure 5.2b). We expect from this SSH restoring in the Atlantic buffer zone to constrain the horizontal pressure gradients at the entrance of the Strait of Gibraltar.

GLORYS-1 anomalies have an amplitude of about 14 cm, in agreement with AVISO products (*Rio et al.*, 2007) which were assimilated in it (Figure 5.2a). During the 2002-2008 period, the correlation between these two times-series (84 monthly values) is 0.94 . The amplitude of the interannual variations are of the order of 2 to 4 cm in both products. The AVISO products used here are the weekly Maps of Absolute Dynamic Topography (MADT), equivalent to the SSH from an oceanic model. These MADTs are built by adding weekly satellite Sea Level Anomalies (SLA) to a reference Mean Dynamic Topography (MDT).

5.1.3 Global validation of the circulation in the Western Mediterranean

In this subsection, we will focus on the Western Mediterranean and on the winter 2005. After a validation of the exchanges at the Strait of Gibraltar in all simulations and of the SSH variability in MED12-ARPERA-3, we describe the general features of temperature, salinity, and the deep convection in the Gulf of Lions, in particular in winter 2005.

5.1.3.1 Modification of the exchanges through the Strait of Gibraltar

We expect from the new implemented parameterizations to mainly play a role on the exchanges between the Atlantic buffer zone and the Mediterranean Sea through the Strait of Gi-

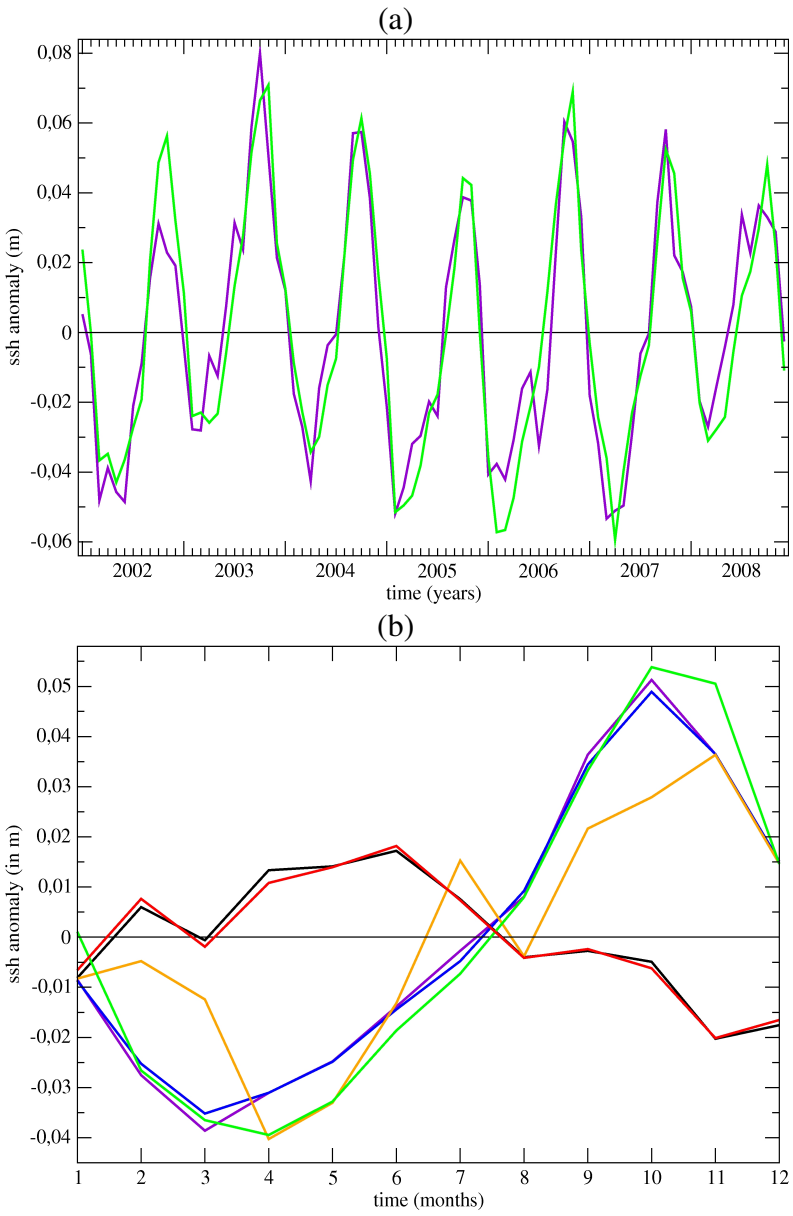

FIG. 5.2 – *Monthly Sea Surface Height anomaly (m) averaged over the area [11-7.5°W, 32-39°N] (ABZ in Figure 5.1) calculated by substracting the 2002-2008 SSH mean for each dataset :*
(a) for the period 2002-2008, interannual (84 monthly) values of (purple) GLORYS-1 are compared to (green) AVISO.
(b) in average for the period 2002-2008, monthly climatological values are compared between datasets : (black) MED12-ARPERA-1, (red) MED12-ARPERA-2, (blue) MED12-ARPERA-3, (purple) GLORYS-1 and (green) AVISO. In orange is added the climatological anomalies of SSH which are used in MED12-ARPERA-3 during the 1998-2001 period.

braltar. Figure 5.3 displays the monthly and annual averages of the net water, heat and salt fluxes through the Strait of Gibraltar. Positive values mean gains for the Mediterranea Sea. For the three fluxes, differences between simulations MED12-ARPERA-1 and MED12-ARPERA-2 are hardly noticeable ; all changes in the outflow are compensated by changes in the inflow, and the annual values of the net heat, salt and water fluxes are very close (Table 5.2). The impact of the new bottom friction is very small on the monthly cycle of the fluxes through the

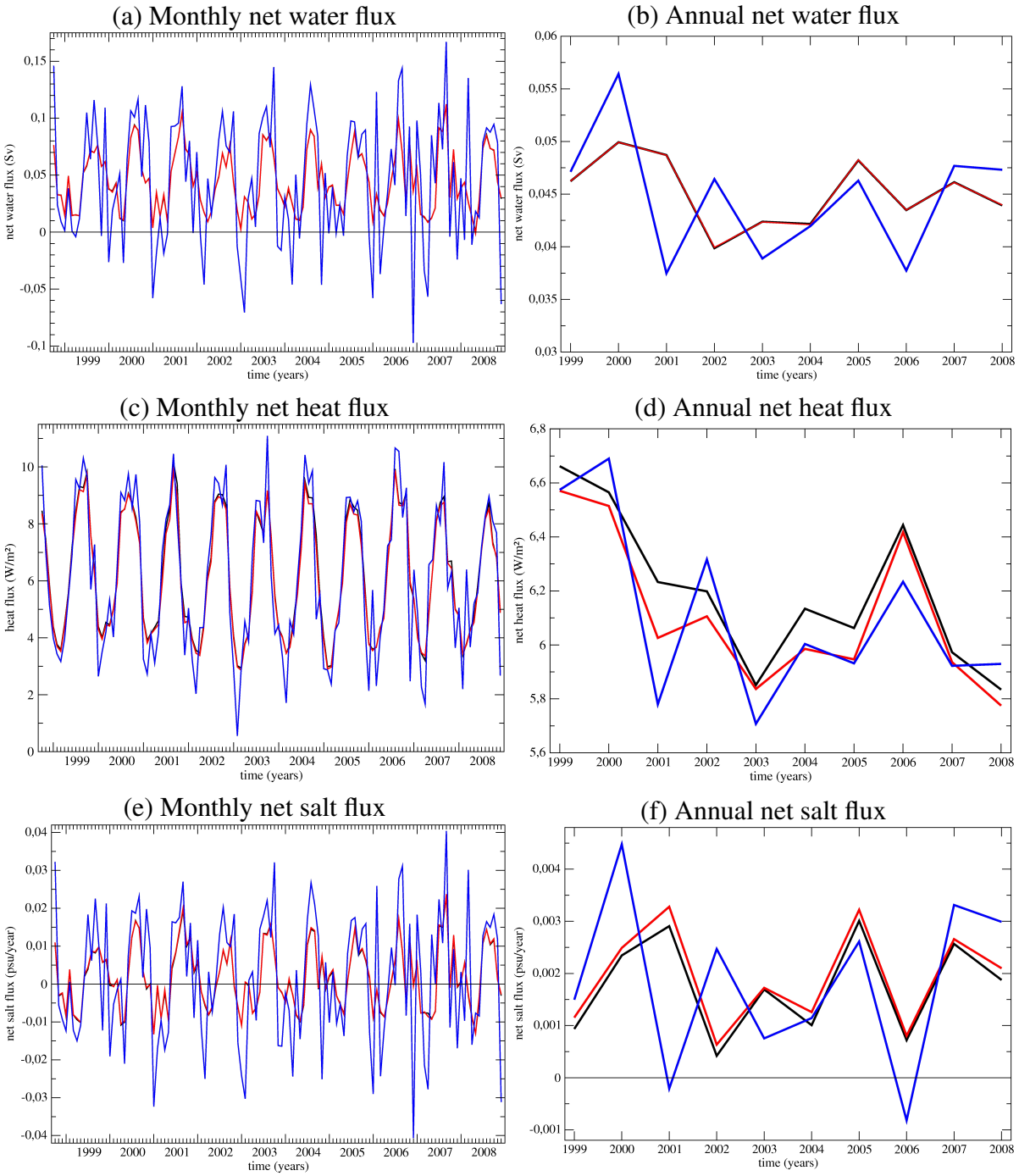

FIG. 5.3 – *Net fluxes towards the Mediterranean Sea through the Srait of Gibraltar for (black) MED12-ARPERA-1, (red) MED12-ARPERA-2 and (blue) MED12-ARPERA-3 : (a, c, e) monthly and (b, d, f) annual averages of the net water flux (a and b, in Sv), the net heat flux (c and d, in W.m^{-2}) and the net salt flux (e and f, in psu.yr^{-1}).*

Strait of Gibraltar. The major differences are seen between the simulation MED12-ARPERA-3 and the other two simulations. For the net water flux, the seasonal cycle amplitude is enhanced in MED12-ARPERA-3 : for the three simulations, the net inflow is maximum in summer and fall seasons, with higher values for MED12-ARPERA-3 (between +0.10 Sv and +0.15 Sv), and minimum in winter and spring seasons, with lower values in MED12-ARPERA-3 (between -0.10 Sv and -0.02 Sv), to such an extent that there is every year a net outflow from the Mediterranean in average during these two seasons (Figure 5.3a), which hardly ever occurs in simulations MED12-ARPERA-1 and MED12-ARPERA-2. The increases of the seasonal cycle amplitude of the net heat and salt fluxes are correlated with those of the net water flux (Figure 5.3b and 5.3c).

The 10-year averages of the net fluxes are very close between the three simulations, but the

Simulation	Water flux (Sv)	Heat flux ($W.m^{-2}$)	Salt flux (10^{-3} psu.yr^{-1})
	Inflow		
MED12-ARPERA-1	$+0.74 \pm 0.04$	$+20.94 \pm 1.05$	$+222 \pm 11$
MED12-ARPERA-2	$+0.73 \pm 0.04$	$+20.63 \pm 1.03$	$+218 \pm 11$
MED12-ARPERA-3	$+0.73 \pm 0.04$	$+20.62 \pm 1.05$	$+218 \pm 11$
	Outflow		
MED12-ARPERA-1	-0.70 ± 0.04	-14.75 ± 0.77	-220 ± 12
MED12-ARPERA-2	-0.69 ± 0.04	-14.52 ± 0.75	-217 ± 11
MED12-ARPERA-3	-0.69 ± 0.04	-14.51 ± 0.74	-217 ± 11
	Net		
MED12-ARPERA-1	$+0.045 \pm 0.003$	$+6.20 \pm 0.29$	$+1.7 \pm 0.9$
MED12-ARPERA-2	$+0.045 \pm 0.003$	$+6.11 \pm 0.29$	$+1.9 \pm 1.0$
MED12-ARPERA-3	$+0.045 \pm 0.006$	$+6.11 \pm 0.33$	$+1.8 \pm 1.6$

TAB. 5.2 – *10-year averages and standard deviations of the inflowing, outflowing and net fluxes towards the Mediterranean Sea through the Strait of Gibraltar, for the three simulations : water flux (in Sv), heat flux (in $W.m^{-2}$) and salt flux (in 10^{-3} psu.yr^{-1}) .*

interannual variability amplitude of the net water flux is twice larger in MED12-ARPERA-3 than in the other two simulations. The values for the mean water fluxes are in the lower part of the range given in the literature : between +0.72 and +1.01 Sv for the inflow, between -0.68 and -0.97 Sv for the outflow and between +0.04 and +0.13 Sv for the net flow (*Bryden and Kinder*, 1991; *Bryden et al.*, 1994; *Tsimplis and Bryden*, 2000; *Candela*, 2001; *Baschek et al.*, 2001; *Lafuente et al.*, 2002). The interannual variations for such a short period are in agreement with *Soto-Navarro et al.* (2010), who estimate the water outflow during the 2004-2009 period with currentmeter observations. They give values of $+0.81 \pm 0.06$ Sv for the water inflow, -0.78 ± 0.05 Sv for the water outflow and $+0.038 \pm 0.007$ Sv for the net water flow. For the net water flow variability, simulation MED12-ARPERA-3 is thus closer to recent observations than the other two simulations, which cannot be discriminated. For the mean values of the net heat flux, there is no difference between the simulations and the values are in the range of the estimations of *Béthoux* (1979) ([4 ; 10] $W.m^{-2}$) and of *Macdonald et al.* (1994) ([3.9 ; 6.5] $W.m^{-2}$). For the net salt flux, the 10-year mean values are close in the three simulations, MED12-ARPERA-3 having a higher interannual variability, obvious in Figure 5.3f.

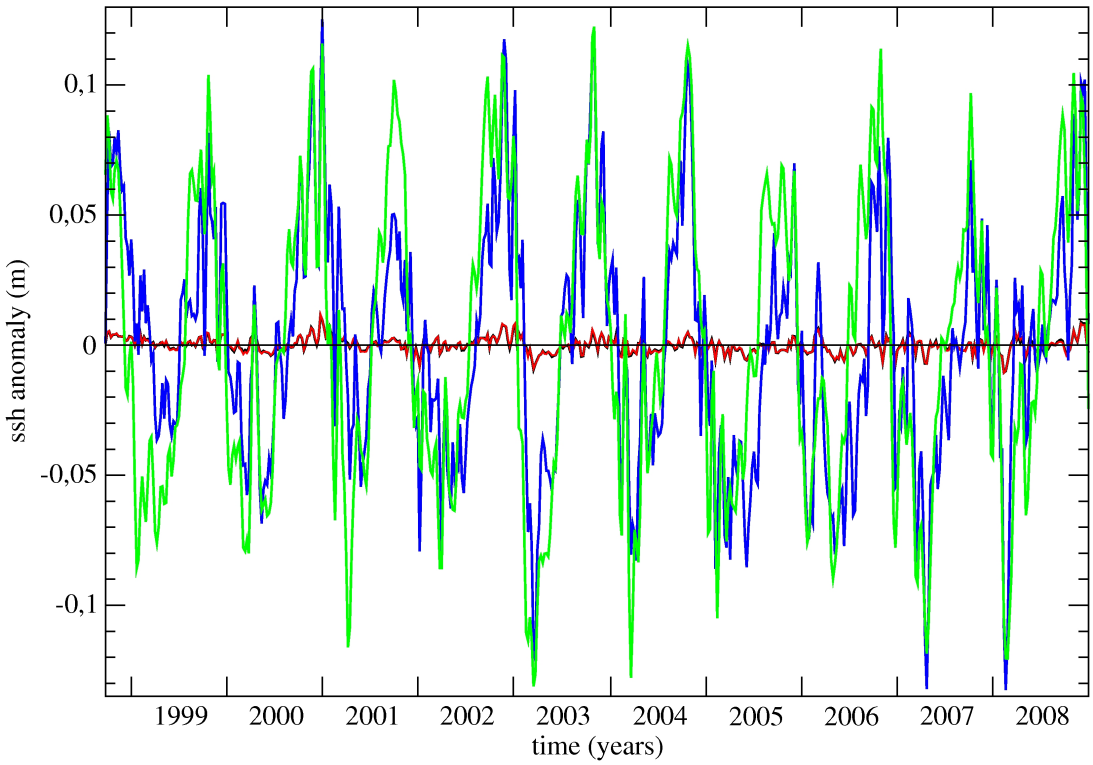

FIG. 5.4 – *Weekly SSH anomalies (m) averaged over the Mediterranean Sea during the 10-year studied period for (black) MED12-ARPERA-1, (red) MED12-ARPERA-2, (blue) MED12-ARPERA-3 and (green) AVISO. For each dataset, anomalies are computed around the average from October 1998 to December 2008.*

5.1.3.2 Improvment of the SSH variability

To estimate the impact of the SSH restoring in the Atlantic area applied in MED12-ARPERA-3, we first look at the SSH averages over the Mediterranean Sea for the three companion simulations and at the weekly MADTs of AVISO (Figure 5.4). The peak-to-peak amplitude of the SSH variations are of the order of those of AVISO only in MED12-ARPERA-3 (26 cm) whereas they are ten times lower in MED12-ARPERA-1 and MED12-ARPERA-2 (2 cm). The correlation between AVISO and MED12-ARPERA-3 time-series (computed with the 536 de-trended weekly values) is 0.83 whereas it is less than 0.53 between AVISO and each of the other two simulations. The changes in the bottom friction do not affect, in average over the all Mediterranean Sea, the SSH variability. On the contrary, the parameterization of the volume conservation through a damping on SSH in the Atlantic area highly improves the modelling of the seasonal SSH cycle in the Mediterranean Sea in average. This improvment is explained by the better physical consistance of a SSH damping in MED12-ARPERA-3 than the one of the water redistribution done in MED12-ARPERA-1 and MED12-ARPERA-2. In reality, the water evaporated over the Mediterranean Sea does not go back instantaneously in the ocean, and moreover it does not go all in the near Atlantic ocean. Thus, the seasonal cycle of the near Atlantic sea level in simulations MED12-ARPERA-1 and MED12-ARPERA2 is the seasonal cycle of the Mediterranean freshwater budget, which has no physical sense. By doing a SSH restoring in the buffer zone, we apply there the seasonal cycle of the water mass in this area, which explains the better agreement with sea level observations. The amplitude of the Mediterranean SSH is also in better agreement for simulation MED12-ARPERA-3 thanks to the good amplitude of the prescribed

SSH in the Atlantic buffer zone, which contains the effect of the steric and mass variations at global scales.

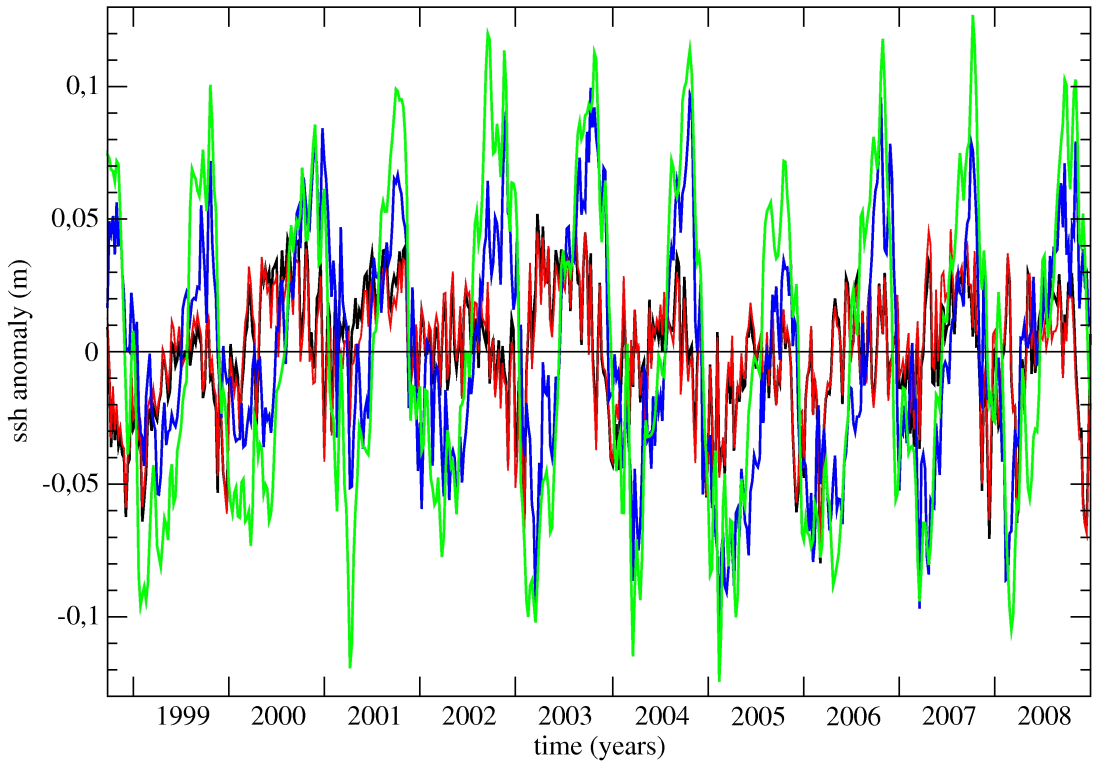

FIG. 5.5 – *Weekly SSH anomalies (m) averaged over the North-Western Mediterranean (NW-MED in Figure 5.1), for (black) MED12-ARPERA-1, (red) MED12-ARPERA-2, (blue) MED12-ARPERA-3 and (green) AVISO. For each dataset, anomalies are computed around the average from October 1998 to December 2008.*

The same result holds for the north-western Mediterranean (Figure 5.5). In MED12-ARPERA-3 (blue line), the variations of the SSH better follow the observed variations than in the other two simulations (black and red lines). The amplitude and the chronology of the SSH variations are in better agreement with AVISO in MED12-ARPERA-3. For this area, the correlation between AVISO and MED12-ARPERA-3 time-series (computed with the 536 de-trended weekly values) is 0.87 whereas it is less than 0.22 between AVISO and each of the other two simulations. The changes in the bottom friction have no significant effect on the modelling of the variation sof the SSH, in average over the Western basin. On the contrary, the SSH damping in the Atlantic area improved the general circulation in the north-western Mediterranean too. In particular, looking at the winter 2005, we can see a period of low SSH, which appears to be longer and stronger than other winters in AVISO and MED12-ARPERA-3. This is linked to the intense winter convection which occurred in the Gulf of Lions (*Schroeder et al.*, 2008; *Herrmann et al.*, 2010). The cyclonic gyre in the Gulf of Lions was enhanced and thus caused a low SSH signature.

We compare the surface circulation in February 2005 in the western Mediterranean for MED12-ARPERA-3 and AVISO (Figure 5.6). The main patterns of the circulation are well reproduced. The surface circulation is cyclonic with the AW which enters the Mediterranean Sea through the Strait of Gibraltar. The two anti-cyclonic gyres in the Alboran Sea are present,

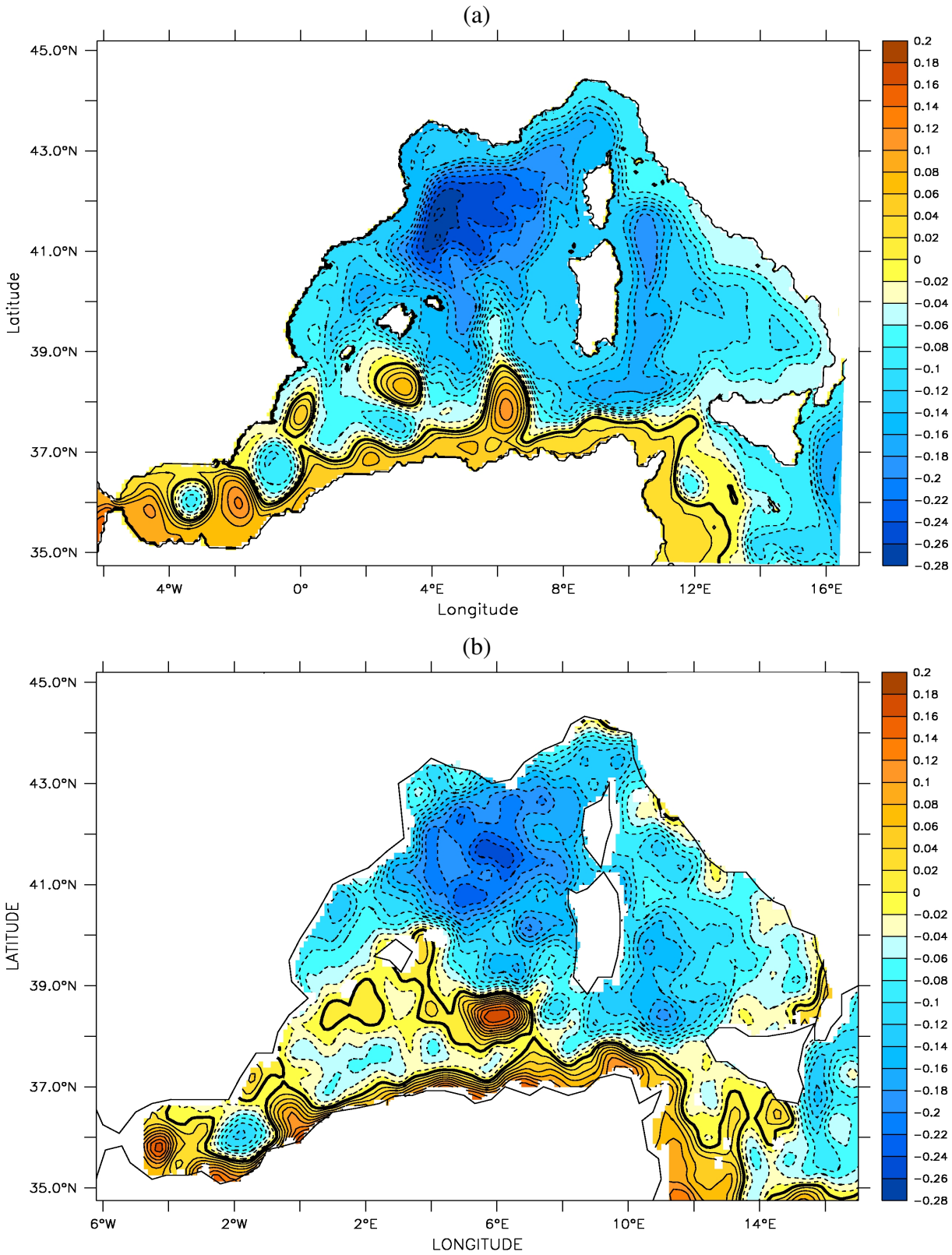

FIG. 5.6 – *Monthly mean of the SSH (m) over the Western Mediterranean, for February 2005, (a) for simulation MED12-ARPERA3 and (b) for AVISO. Contours are every 0.02 m, with dashed lines for negative values (cyclonic) and full lines for positive values (anticyclonic).*

even if their locations differ a little between the model and the observations. Then the shallow

Algerian Current flows eastwards along the African coast and anticyclonic eddies more or less detached from the coast are depicted. Anticyclonic areas near 2 °E and 6 °E at around 38 °N are in agreement in both products. The Algerian Current crosses then the Channel of Sardinia and splits in several branches at the level of the Channel of Sicily. One branch enters the Tyrrhenian Sea and circulates along the Italian coast before crossing the Strait of Corsica, generating there part of the Northern Current. This current then partly retroflects near 4 °E to form the cyclonic gyre of the Gulf of Lions, well marked in February 2005. It is centered near 42 °N - 4 °E in the model and near 41.5 °N - 6 °E in the observations. The SSH in the gyre of the Gulf of Lions is of the order and lower than -20 cm for both products in the area [40 - 43 °N ;3 - 8 °E]. A part of the Northern Current flows southwestwards off the Balearic islands.

5.1.3.3 Global thermohaline characteristics of the Western Mediterranean

To study the representativity of the interannual variability in the simulations in the Western Mediterranean, we discuss the potential temperature and salinity time-series averaged in the Western Mediterranean (Figure 5.7), which is between the Strait of Gibraltar and the Channel of Sicily.
The average potential temperature of the Western Mediterranean varies between 13.10 and 13.45 °C ($\Delta\theta \sim 0.35$ °C) with well marked seasonal and interannual variations (Figure 5.7a). These values are close to those of the climatology of *Rixen et al.* (2005), which gives θ between 13.08 and 13.28 °C for this period. Potential temperature differences between the three companion simulations are very small (lower than 0.01 °C), in spite of the differences noticed in the net heat flux at the Strait of Gibraltar. This is due to the use of the SST retroaction in the atmospheric surface heat flux for the three simulations, which tends to reduce any deviation from the same observed SST field. Very cold winters like those of 1999, 2005 and 2006 are identified by the lowest potential temperature values (below 13.15 °C in winter), while other years can be considered as relative warm winters, especially 2007 and 2008 for which the minimum value is higher than 13.2 °C in winter.
The average salinity of the Western Mediterranean varies between 38.415 and 38.445 psu ($\Delta S \sim$ 0.03 psu) with alternative periods of salinity decreases and increases (Figure 5.7b). The salinity decrease of 1999-2001 is in agreement with *Rixen et al.* (2005), as the range of the values and of the interannual variability (S is between 38.37 and 38.46 psu for those years). Salinity differences between the companion simulations are lower than 0.007 psu and can be explained by the differences noticed in the salt fluxes through the Strait of Gibraltar. And, as no SSS damping is used, the variations in the salt exchanges at the Strait of Gibraltar can develop freely and in different ways between the three simulations, unlike for the potential temperature.

Deep convection occurs in the Gulf of Lions during the 10-year period as deduced from the time-series of the daily spatial maximum reached by the convection in Figure 5.8a. In particular, the convection reaches depths higher than 2000 m depth for events longer than two months in 2000, 2004 and 2006, and longer than a month and a half from end January to early March 2005. Deeper convection occurs in MED12-ARPERA-3 compared to other simulations in 2001 and 2002, but the deep convection event lasts a very short time and is localized in a single small chimney (not shown). We also note that no deep convection occurs in 2007 and 2008 in the simulations. These time-series are in agreement with another modelling work obtained after a 15-year spin-up (*Béranger et al.*, 2009) and thus this shows some skills of such short simulations to represent the interannual variability of the general circulation. Looking at the evolution of the volume of dense waters in the north-western Mediterranean (Figure 5.8b), we identify the WMDW with the usual density threshold of 29.10 $kg.m^{-3}$, but we also use denser thresholds to

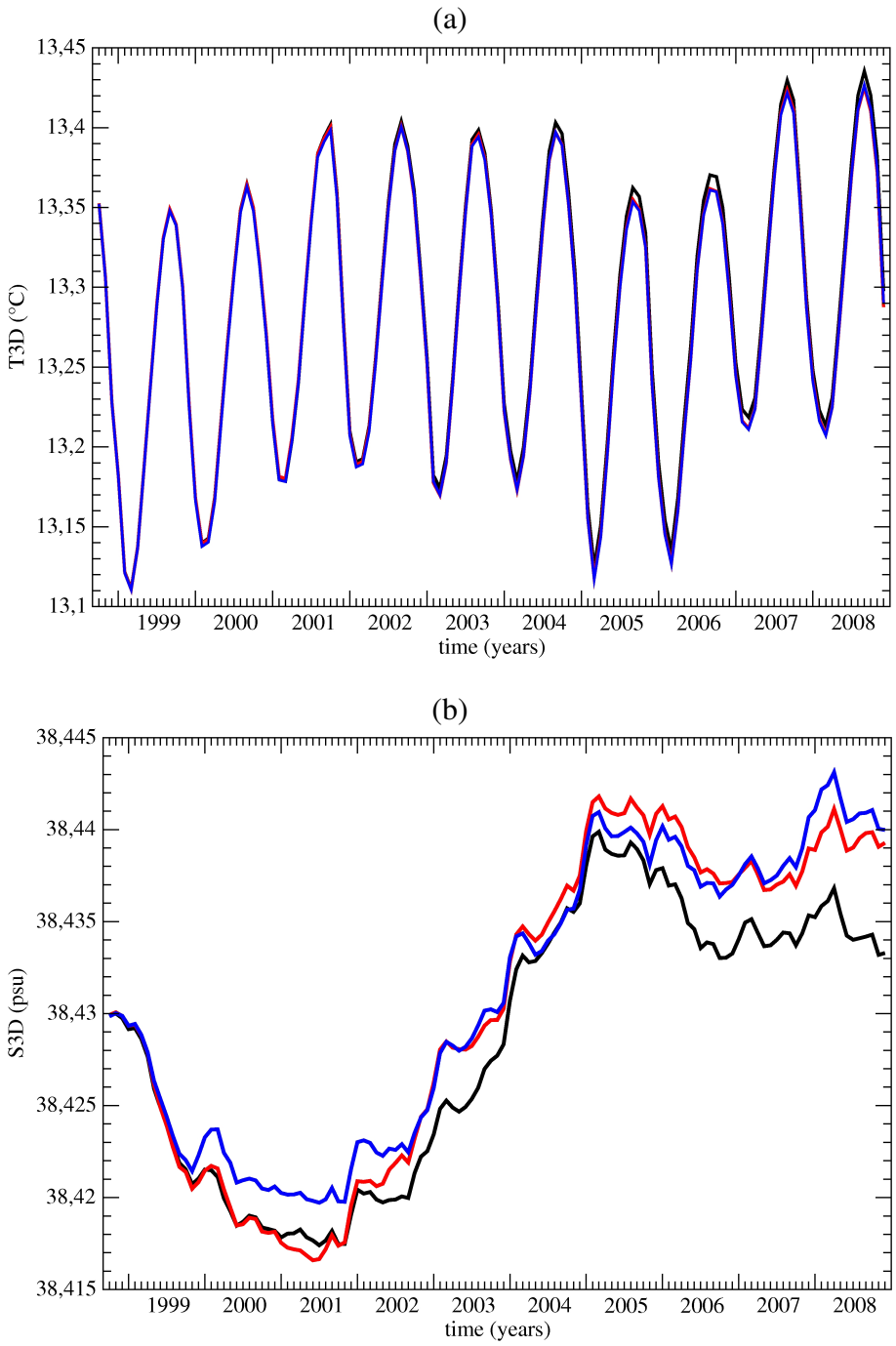

FIG. 5.7 – *Monthly time-series, from October 1998 to December 2008, of (a) the potential temperature (T3D in °C) and (b) the salinity (S3D in psu) averaged over the Western Mediterranean, for (black) MED12-ARPERA-1, (red) MED12-ARPERA-2 and (blue) MED12-ARPERA-3.*

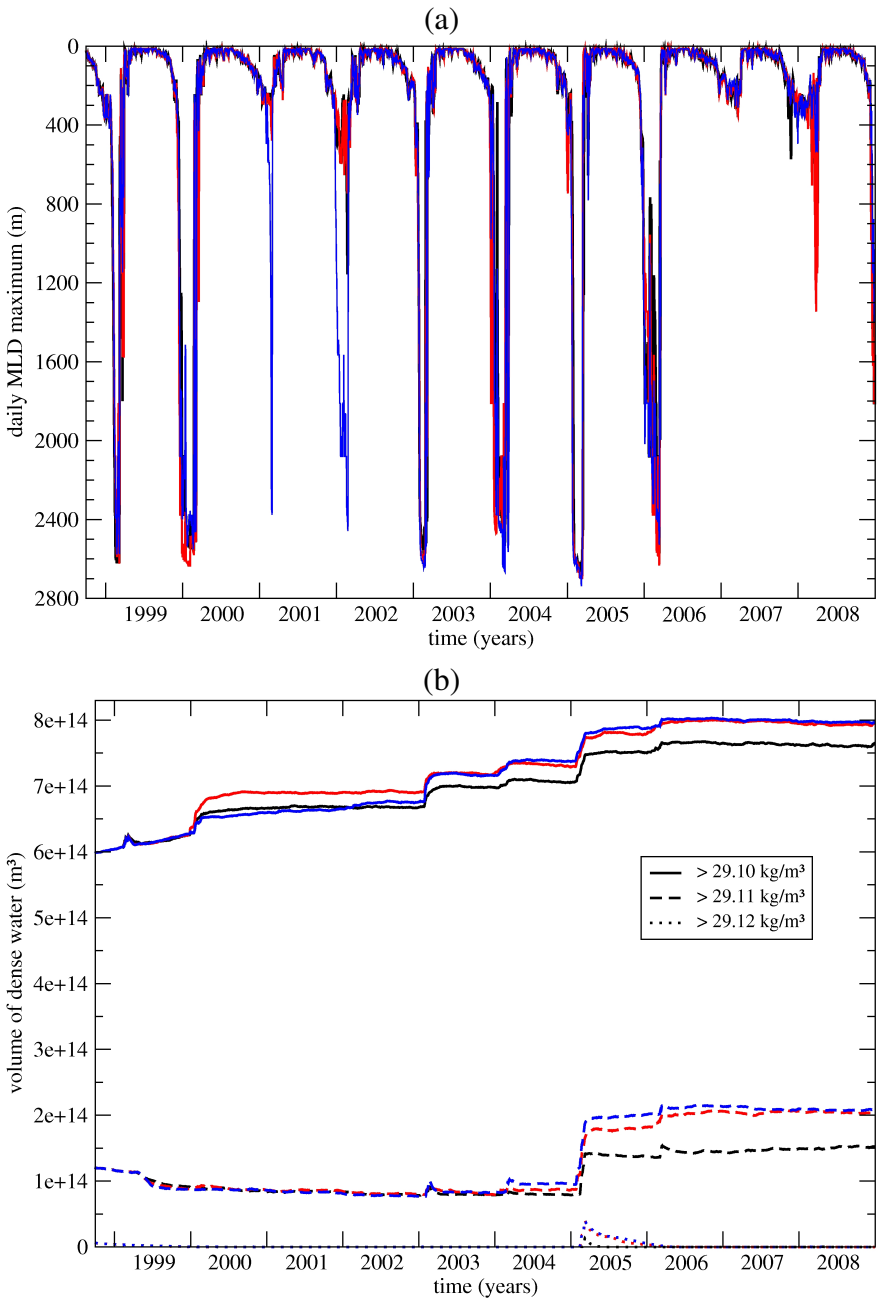

FIG. 5.8 – *Daily values, from the 1st October 1998 to the 1st December 2008, of (a) the maximum of the turbocline depth (m) in the* ***North-Western Mediterranean*** *(cf. Figure 5.1), and (b) the volume (in m^3) of dense waters in the* ***Western Mediterranean*** *for three thresholds : denser than 29.10 (solid lines), 29.11 (dashed lines) and 29.12 kg.m^{-3} (dotted lines). MED12-ARPERA-1 is in black, MED12-ARPERA-2 in red and MED12-ARPERA-3 in blue.*

Simulation	MED12-ARPERA-1			MED12-ARPERA-2			MED12-ARPERA-3		
Class / Winter	2005	2006	Mean	2005	2006	Mean	2005	2006	Mean
$\geq 29.10\,kg.m^{-3}$	1.26	0.48	0.87	1.30	0.52	0.91	1.26	0.42	0.84
$\geq 29.11\,kg.m^{-3}$	2.08	0.52	1.30	2.85	0.51	1.68	3.05	0.41	1.73
$\geq 29.12\,kg.m^{-3}$	0.44	0.00	0.22	1.27	0.03	0.65	1.26	0.00	0.63
$\geq 29.13\,kg.m^{-3}$	0.02	0	0.01	0.14	0	0.07	0.28	0	0.14

TAB. 5.3 – *Dense water formation rates (in Sv) in the Gulf of Lions for winters 2005 and 2006 for the three companion simulations.*

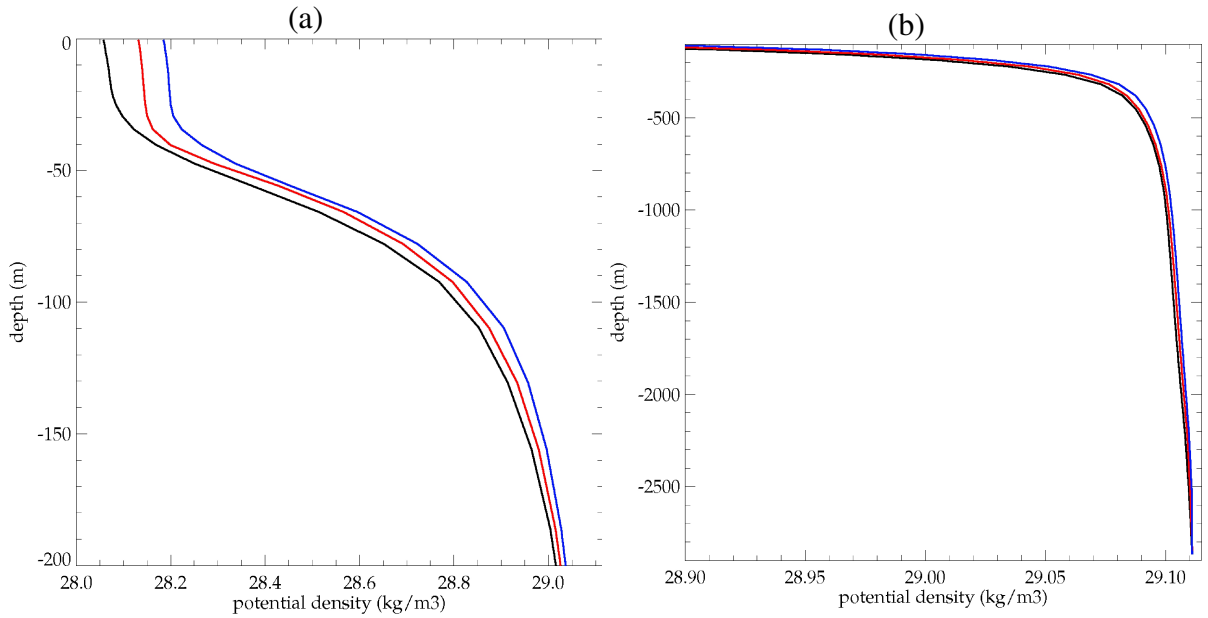

FIG. 5.9 – *Vertical profiles of the potential density (in kg.m^{-3}), in average for the Gulf of Lions (see Figure 5.1) and for November 2004 : (a) from the sea surface to 200 m depth and (b) from 100 m depth to the sea bottom. MED12-ARPERA-1 is in black, MED12-ARPERA-2 in red and MED12-ARPERA-3 in blue.*

highlight the exceptionality of winter 2005 and to better identify the new WMDW. Water denser than 29.10 kg.m^{-3} is formed during winters 1999, 2000, 2003, 2004, 2005 and 2006. Water denser than 29.11 kg.m^{-3} is formed during winter 2005 in larger quantities compared to winters 2003, 2004 and 2006. Water denser than 29.12 kg.m^{-3} is only formed, in sizeable amount, during winter 2005. And in early March 2005, water denser than 29.13 kg.m^{-3} is formed, mainly in simulations MED12-ARPERA-2 and MED12-ARPERA-3 (not shown on Figure 5.8b, see Table 5.3). Thus, the 29.11 kg.m^{-3} can be used to characterise the new WMDW and its formation rate.

The change in the bottom friction parameterization increases the formation of water denser than 29.10 kg.m^{-3} in winter 2000 and of water denser than 29.11 kg.m^{-3} in winter 2005 in MED12-ARPERA-2 compared to MED12-ARPERA-1. The change in the SSH condition in the Atlantic area reduces the dense water formation of water denser than 29.10 kg.m^{-3} in winter 2000 in MED12-ARPERA-3 compared to MED12-ARPERA-2, but increases it in winter 2003 for water denser than 29.10 kg.m^{-3} and in winter 2004 for water denser than 29.11 kg.m^{-3}. The changes of the AW inflow at the level of the Strait of Gibraltar has drastic consequences on the

thermohaline circulation in the Gulf of Lions as argued by *Sannino et al.* (2009). We showed in Figure 5.3 that the variability of the heat and salt fluxes entering the Western Mediterranean through the Strait of Gibraltar differs between the three simulations, modifying the variability of the Western Mediterranean heat and mostly salt contents (Figure 5.7). It leads to a variable intensity of the deep convection in the Gulf of Lions in the three simulations (Figure 5.8). As a consequence, in November 2004, the whole water column in average in the Gulf of Lions is denser at all level in MED12-ARPERA-3 than in MED12-ARPERA-1 and MED12-ARPERA-2. At the sea surface, MED12-ARPERA-3 is denser than MED12-ARPERA-2 by $\sim 0.05\,\mathrm{kg.m^{-3}}$ and than MED12-ARPERA-1 by $\sim 0.12\,\mathrm{kg.m^{-3}}$ (Figure 5.9a). The gap slightly decreases with the depth, but MED12-ARPERA-3 remains denser than the other two simulations in all the water column (Figure 5.9b). With the same atmospheric forcings, it leads to a higher volume of very dense water formed in MED12-ARPERA-3. For winter 2005, associated formation rates are gathered in Table 5.3. MED12-ARPERA-3 gives formation rates slightly higher than the other two simulations. To compare our results with the 2.4 Sv mean estimate over the two winters 2005 and 2006 of *Schroeder et al.* (2008), derived from the volumetric distribution of the θ-S properties in in-situ observations for the end 2004 - end 2006 period, we add in Table 5.3 the dense water formation rates for winter 2006. With the 29.11 threshold, it gives a mean formation rate over these two winters of 1.30, 1.68 and 1.73 Sv for the three companion simulations respectively. We thus argue that MED12-ARPERA-3 is slighlty closer to the estimate made by *Schroeder et al.* (2008) than the other two simulations. In comparison, for the single winter 2005, *Béranger et al.* (2009) and *Herrmann et al.* (2010) obtained a formation rate of 1.28 Sv and 1.16 Sv respectively, $i.e.$ 2.5 times lower than in MED12-ARPERA-3 (3.05 Sv).

The exceptional winter convection event in 2005 gives the largest volume of dense water formed compared to the 10-year studied period and other estimates reported in *Marshall and Schott* (1999). It is also exceptional in terms of spatial extent of the deep convection area. Figure 5.10 compares the maximal extent of the $29.10\,\mathrm{kg.m^{-3}}$ isopycne at surface for the 10 winters simulated in MED12-ARPERA-3 (in winters 2007 and 2008, this isopycne does not reach the surface of the sea). Winter 2005 appears to have the widest convection area (about $48000\,\mathrm{km^2}$, see Table 5.4), in the open sea (from the usual location of $42\,^{\circ}\mathrm{N} - 5\,^{\circ}\mathrm{E}$) as on the shelf of the Gulf of Lions. The deep convection area extends south-westwards, downstream of the Northern Current towards the Balearic Islands, but also eastwards until $7.5\,^{\circ}\mathrm{E}$. Deep mixed layers have been observed in the eastern Catalan subbasin ($4.845\,^{\circ}\mathrm{E} - 39.785\,^{\circ}\mathrm{N}$, *Smith et al.* (2008)) in early March 2005. The convection area in MED12-ARPERA-3, as identified in winter 2005 in Figure 5.10, clearly extends to the eastern part of the Catalan subbasin (Csb in Figure 5.1), even if it does not reach the far south position observed. During the other winters in this simulation, the convection does not occur in all these parts of the Gulf of Lions, showing again the exceptional intensity of the convection in winter 2005.

For each winter, the day corresponding to the maximal horizontal extent of the $29.10\,\mathrm{kg.m^{-3}}$ isopycne is also indicated in Figure 5.10. Winter 2005 has the latest date for this maximal extent, which occurs on the 7^{th} March 2005. It is an other point that underlines the exceptionality of this winter in terms of duration of the severe winter conditions over the Gulf of Lions, well reproduced in the simulation. The occurence of the maximal extent of the convection area in early March is also consistent with surface chlorophyll concentration observations by MODIS satellite reported in *Herrmann et al.* (2010).

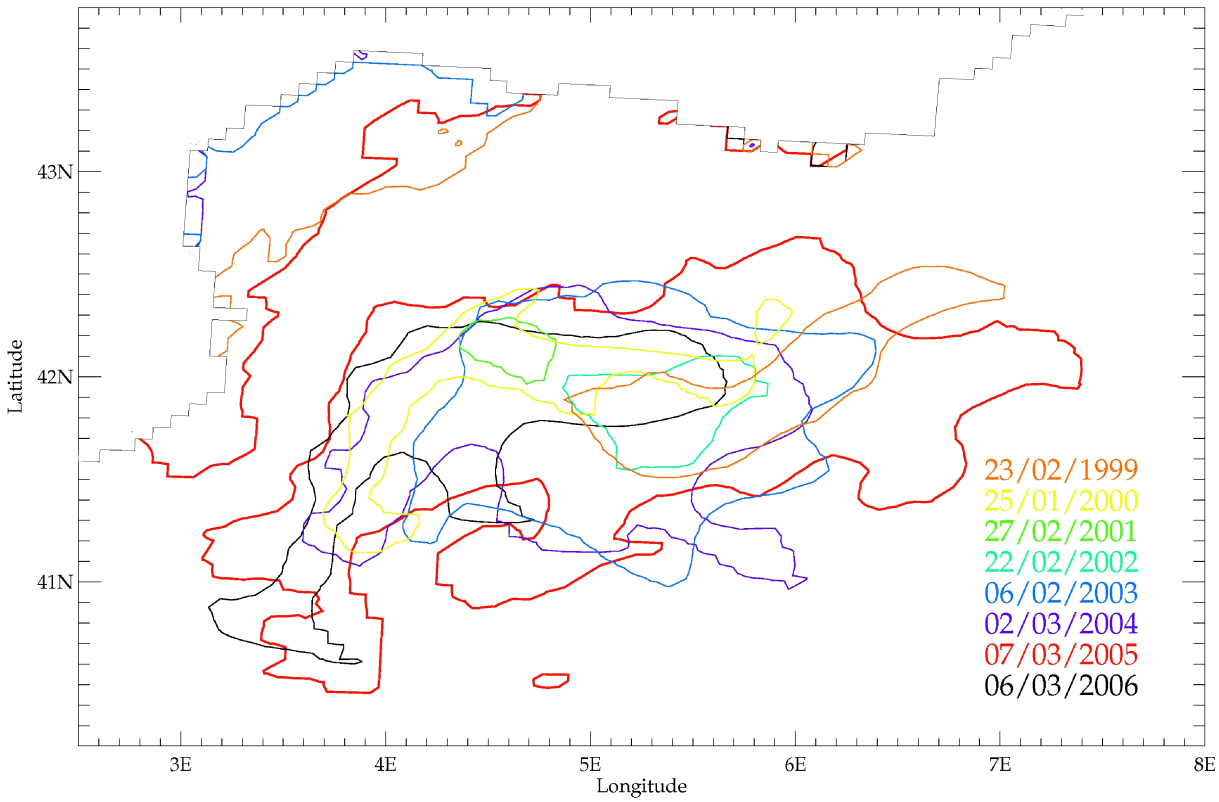

FIG. 5.10 – *Daily maximal extent of the 29.10 kg.m^{-3} isopycne at the sea surface in the Gulf of Lions, in winter 1999 (orange, 23rd February 1999), 2000 (yellow, 25th January 2000), 2001 (green, 27th February 2001), 2002 (turquoise, 22nd February 2002), 2003 (blue, 06th February 2003), 2004 (purple, 2nd March 2004), 2005 (red, 7th March 2005) and 2006 (black, 6th March 2006), in simulation MED12-ARPERA-3. In winters 2007 and 2008, the 29.10 kg.m^{-3} isopycne does not reach the sea surface.*

5.1.4 Spreading of WMDW after winter 2005

In this subsection, we characterise in the model the spreading of the dense water formed in winter 2005, from the convection area in the Gulf of Lions southwards in the Western Mediterranean, and we assess the comparison with in-situ observations made at that time. Then, we adopt successively an eulerian and a lagrangian analysis to estimate the transport time. Since the volume of dense ($\geq$ 29.11) and very dense ($\geq$ 29.13) water formed in winter 2005 is higher in the simulation MED12-ARPERA-3, we use the results of this simulation to better follow the deep spreading of the new WMDW.

5.1.4.1 θ-S characteristics of the new WMDW

The temperature and salinity characteristics of waters denser than 29.10 in the Gulf of Lions are shown in Figure 5.11 for the $1st$ November 2004, the $7th$ March 2005, the $1st$ May 2005 and the $1st$ November 2005. The densest WMDW at the end of 2004, $i.e.$ before the convection event of 2005, is 29.112 kg.m^{-3} (θ = 12.76-12.78 °C, S = 38.440-38.450 psu, Figure 5.11a). During the most intense phase of the deep convection event, the 7th of March 2005 in the model, the new WMDW is characterized by a maximal density of 29.138 kg.m^{-3} (θ = 12.67-12.72 °C, S = 38.440-38.453 psu, Figure 5.11b). Two months later in spring, after the restratification phase, this highest density is still above 29.130 kg.m^{-3} (θ = 12.65-12.71 °C, S = 38.435-

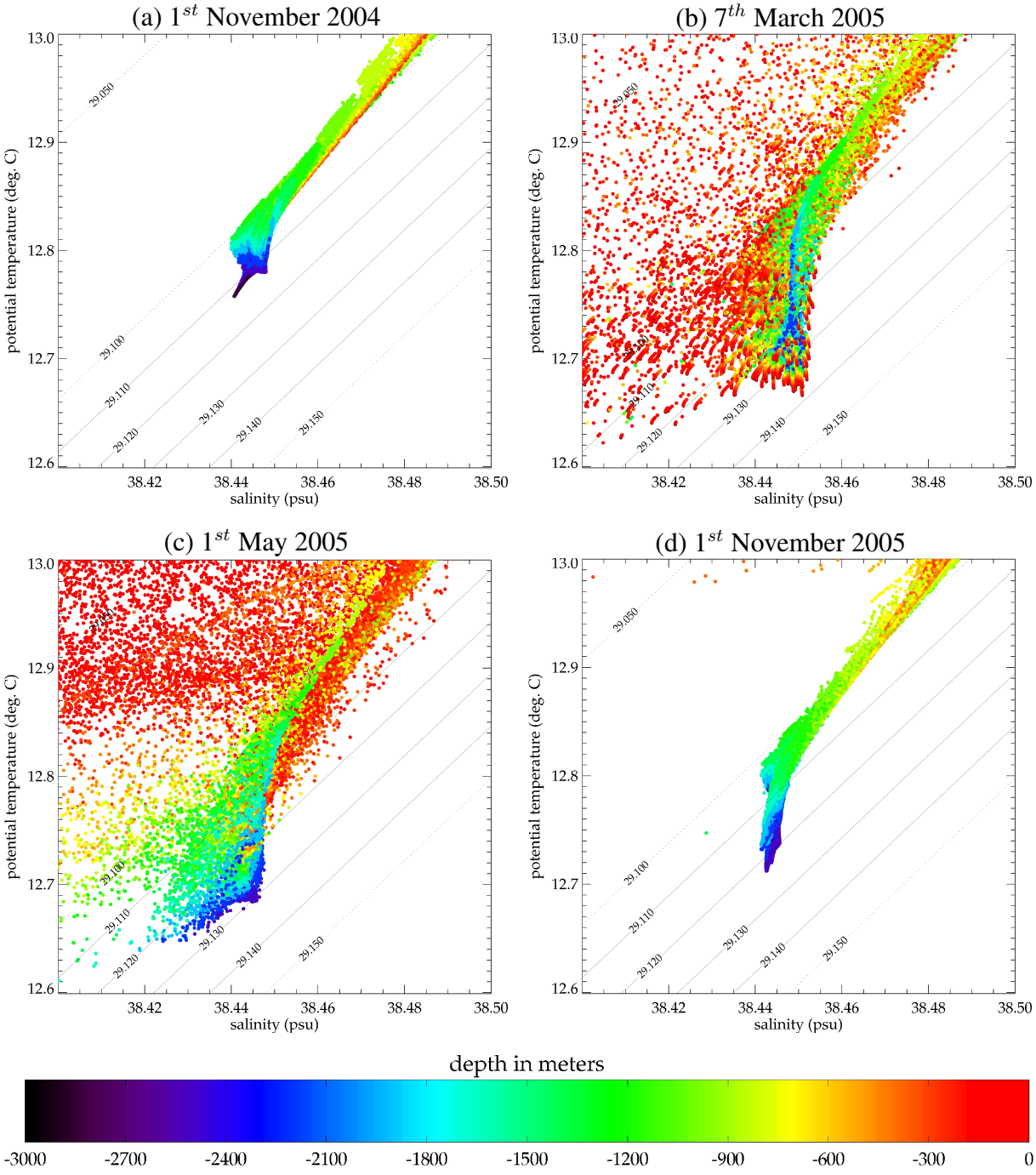

FIG. 5.11 – *θ-S diagrams in the Gulf of Lions, in simulation MED12-ARPERA-3, for (a) the 1st November 2004, (b) the 7th March 2005, (c) the 1st May 2005 and (d) the 1st November 2005. The color of the dots indicates the depth in the model. Thin and dashed lines indicate potential density values in kg.m^{-3}.*

Winter	Maximal extent (km^2)
1999	16694
2000	6918
2001	1130
2002	3222
2003	20889
2004	19351
2005	47968
2006	17432
2007	0
2008	0
10-year average and standard deviation	13360 ± 14031

TAB. 5.4 – *Maximal extent (in km^2) of the area with sea surface density $\geq 29.10\,kg.m^{-3}$ in the north-western Mediterranean (see Figure 5.1 for its boundaries), for the 10 simulated winters in simulation MED12-ARPERA-3. The average and standard deviation of the 10 yearly maxima are also indicated.*

38.448 psu, Figure 5.11c) whereas eight months later it has decreased by about 0.01 $kg.m^{-3}$ in the Gulf of Lion towards 29.123 $kg.m^{-3}$ (θ = 12.70-12.75 °C, S = 38.442-38.448 psu, Figure 5.11d). Compared to observations of *López-Jurado et al.* (2005), *Schröder et al.* (2006), *Font et al.* (2007) and *Smith et al.* (2008), who reported θ = 12.87-12.90 °C and S = 38.47-38.49 psu, the thermohaline characteristics of the new WMDW formed in winter 2005 in the model are not warm enough and not salty enough. Obtaining such an agreement is very difficult with a numerical model, mainly because of uncertainties in the initial conditions, the atmospheric fluxes and the physics of the model. Here, it could be related to the presence or not of dense water formed during the Eastern Mediterranean Transient in the early 1990's (*Roether et al.*, 2007) in the simulation or in the initial conditions only. In fact, *Herrmann et al.* (2010) obtained good θ-S characteristics for the new WMDW with the same atmospheric forcing but with a 46-year simulation, containing thus a simulated EMT. Nevertheless, the density signature is in agreement with observations in our simulation, allowing us to follow the deep water mass propagation in the model.

5.1.4.2 θ-S characteristics in the South of the Western Mediterranean

Following the observations of *Schroeder et al.* (2008), we look at the thermohaline characteristics of waters near the Channel of Sardinia and the Strait of Gibraltar to detect the arrival of the new WMDW at these places. Even if our results are satisfying for the Channel of Sardinia, the model does not succeed in catching such signature at the Strait of Gibraltar. We consider then the θ-S diagram of waters in two boxes (see Figure 5.1), box 1 west of the Channel of Sardinia [8 °E ; 9 °E]-[37 °N ; 39 °N], and box 2 west of the Algerian subbasin [2 °E ; 3 °E]-[36.5 °N ; 39 °N]. In the two boxes, the last point of the θ-S diagrams corresponds to 2530 m depth.

For the Sardinian area (Figure 5.12), there is no change in the deep thermohaline characteristics between the 1^{st}October 2004 (black line) and the 1^{st} December 2005 (dark blue line). A noticeable change starts to appear during December 2005, since the profile of the 1^{st} January 2006 (light blue line) shows waters slightly denser, colder and saltier than the previous one. Then,

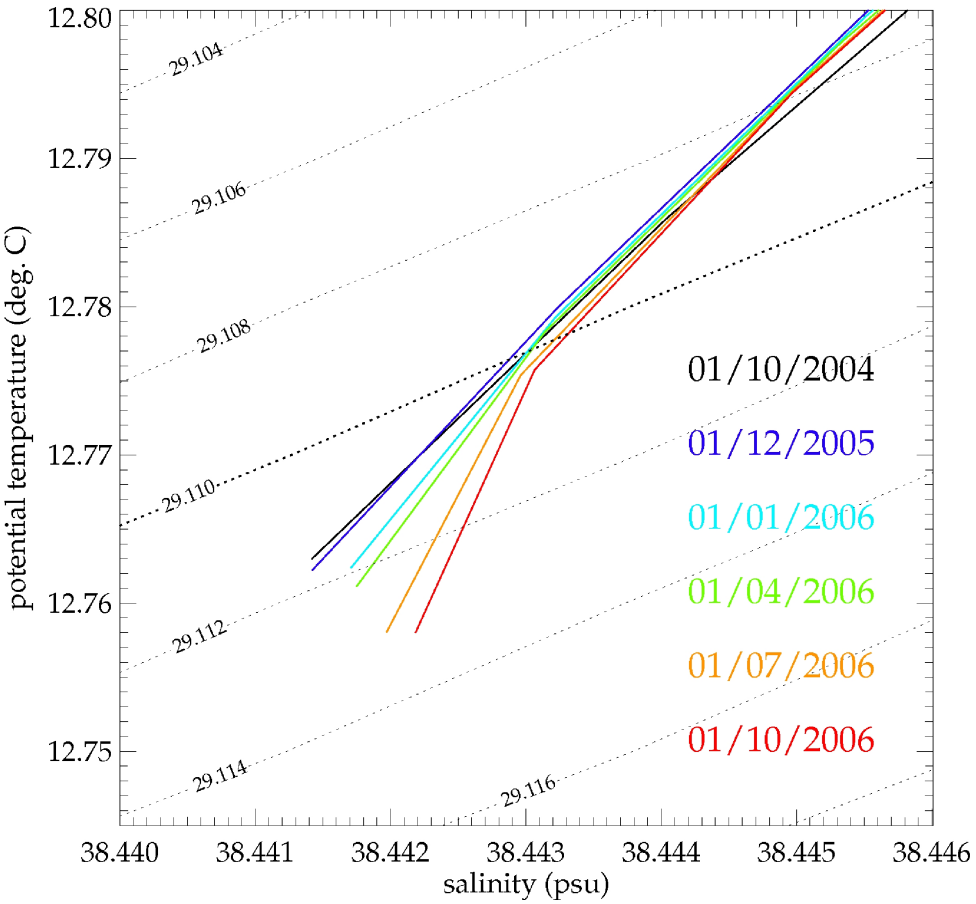

FIG. 5.12 – *Bottom end of θ-S profiles averaged over the box [8°E ; 9°E]-[37°N ; 39°N] (box 1 in Figure 5.1, west of the Channel of Sardinia) in simulation MED12-ARPERA-3. Dashed lines indicate potential density values in kg.m^{-3}. The correspondance between dates and colors is indicated within the diagram.*

these changes continue in the same way and for the 1^{st} October 2006 (red line) the deep water has become denser by 0.002 kg.m^{-3} ($\rho = 29.113$ kg.m^{-3}), colder by 0.005°C ($\theta = 12.758$°C) and saltier by 0.001 psu (S = 38.442 psu) than before. Thus, in the model, it takes about 9 to 10 months (from February-March to December 2005) for the new WMDW to reach the Channel of Sardinia. The signature of this new water mass is relatively weak because the density of old water is initially of 29.111 at this place, which is relatively high but which corresponds to the density of the old WMDW in the Gulf of Lions (as seen in subsection 5.1.4.1). Nevertheless, reminding that it is obtained for very deep water and by averaging over a box of $1° \times 2°$, this signature is noticeable.

For the Algerian area (Figure 5.13), between the 1^{st} October 2004 (black line) and the 1^{st} January 2006 (dark blue line), the slight deep warming and salting associated with a tiny density decrease are certainly caused by mixing or diffusion with water above and not by the advection of a new water mass, since the new WMDW are colder and denser than the old one. Then, the deep thermohaline characteristics of this area remain almost constant until the 1^{st} March 2006 (light blue line). A significant change starts to appear during March 2006, since the profile of the 1^{st} April 2006 (green line) shows waters slightly colder and denser than the previous one. Then, the profile for the the 1^{st} October 2006 (red line) is denser, coldier and saltier than 9 months before, changes and new characteristics being similar as those of the Sardinian area.

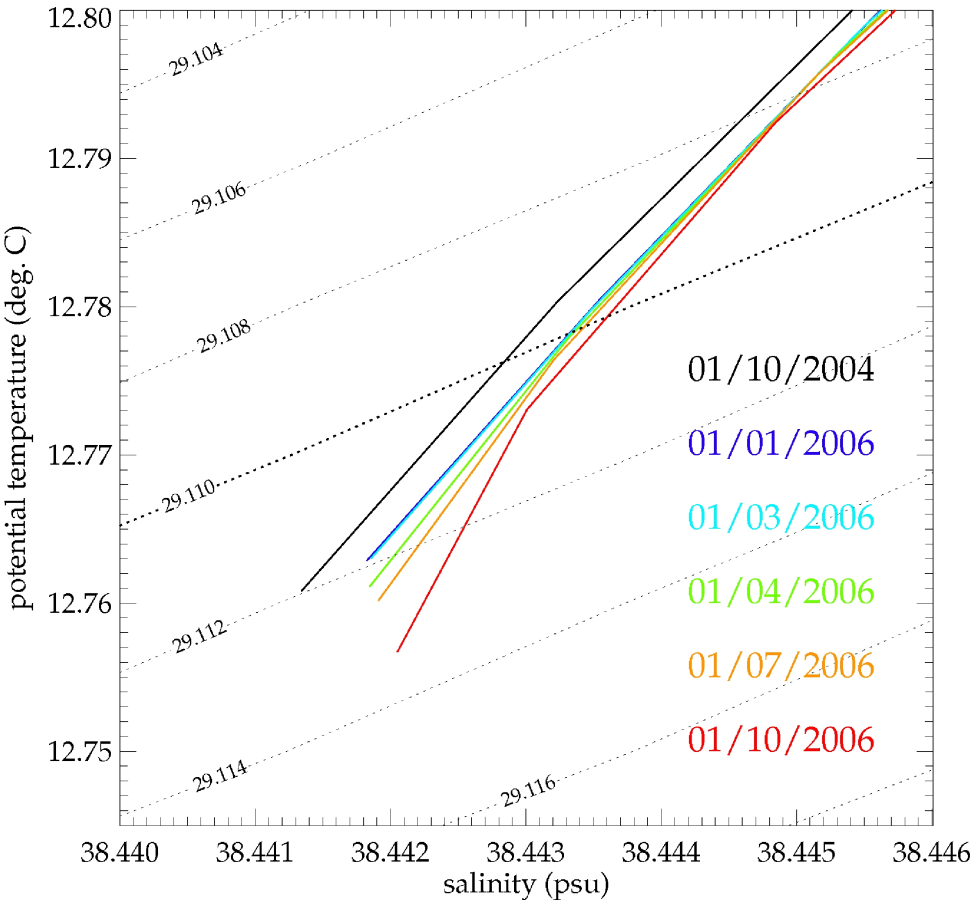

FIG. 5.13 – *Bottom end of θ-S profiles averaged over the box [2°E ; 3°E]-[36.5°N ; 39°N] (box 2 in Figure 5.1, west of the Algerian subbasin) in simulation MED12-ARPERA-3. Dashed lines indicate potential density values in kg.m^{-3}. The correspondance between dates and colors is indicated within the diagram.*

Thus, in the model, it takes about 12 to 13 months (from February-March 2005 to March 2006) for the new WMDW to reach the deep area between the Balearic islands and the Algerian coast.

5.1.4.3 Transport estimates

Eulerian considerations

Using the results of the simulation MED12-ARPERA-3, we follow the deep spreading of the new WMDW formed in winter 2005. As argued in subsection 5.1.3.3, the core of the new WMDW in the model is identified by the 29.11 kg.m^{-3} threshold. The depth of the $\sigma_0 = 29.11$ isopycne (Figure 5.14) is a first way to follow the propagation of the new WMDW. To favour the comparison with observations, we choose the same dates as in *Schroeder et al.* (2008). In October 2004 (Figure 5.14a), the preconditionning due to the cyclonic gyre in the Gulf of Lions is obvious, inducing a doming of the isopycnal surfaces and thus the 29.11 isopycne depth is less than 1600 m in this area. In the other part of the Algero-Provencal subbasin, the isopycnal surface is deeper than 2100 m, and even deeper than 2500 m near the Ligurian subbasin (Lsb in Figure 5.1). There is no water with such a density or denser in the Catalan subbasin (Csb in Figure 5.1) and in the center of the Ligurian subbasin. In June 2005 (Figure 5.14b), *i.e.* 3 months after the end of the deep convection event, the core of the recently formed water mass is located between the Gulf of Lions and the Balearic Islands, and the 29.11 isopycne is shallower

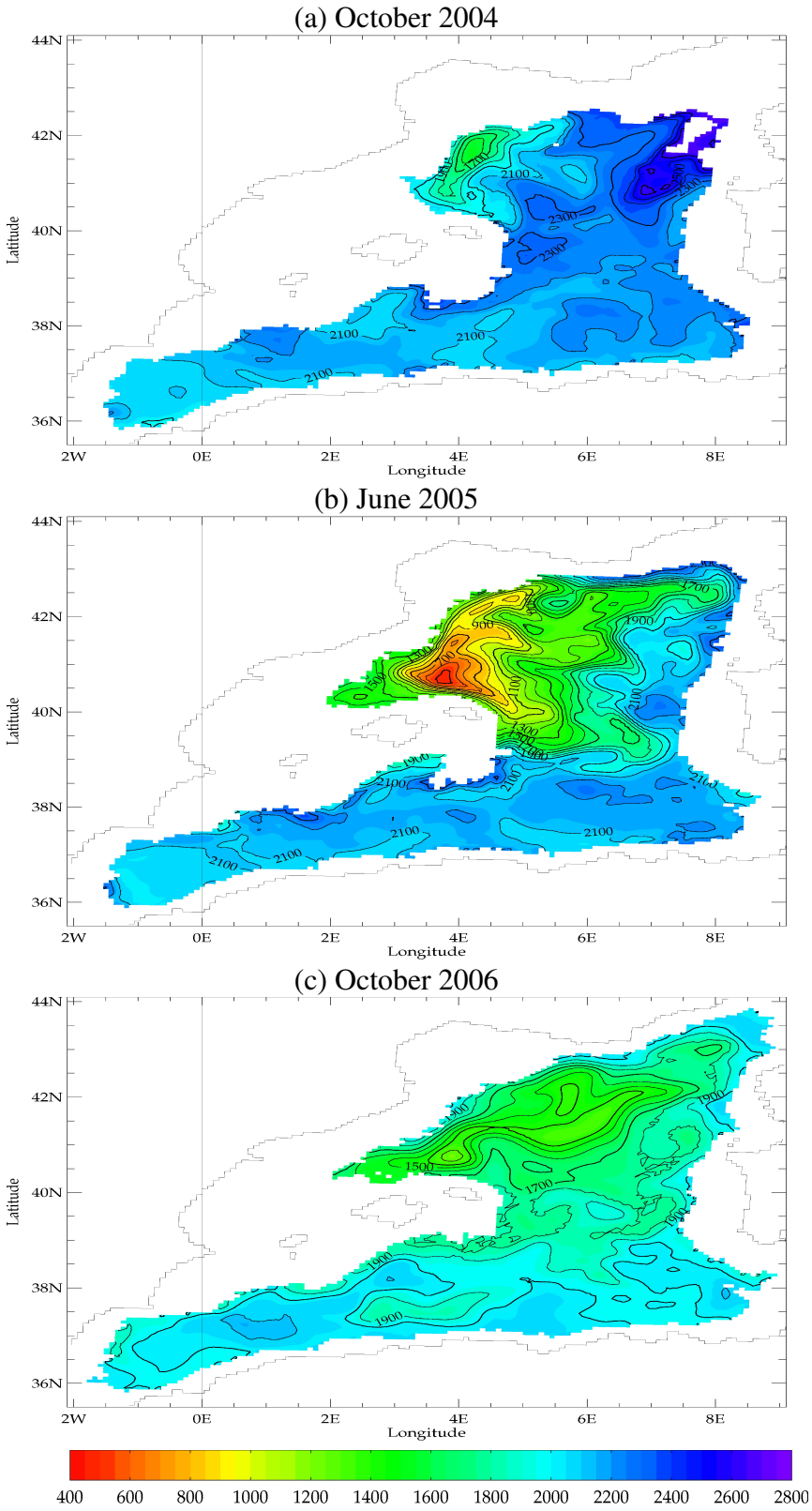

FIG. 5.14 – *Monthly averages of the depth (in meters, contour lines every 100 m) of the $\sigma_0 = 29.11$ isopycnal surface, in simulation MED12-ARPERA-3, for (a) October 2004, (b) June 2005 and (c) October 2006.*

than 500 m. New WMDW is present in the eastern part of the Catalan subbasin (in consistence with the occurence of deep convection in this area, as described in Figure 5.10) and flows along the continental slope off the coast of Minorca Island (easternmost island of the Balearic archipelago). From the convection area, the new WMDW spreads also to the east towards the center of the subbasin. In October 2006 (Figure 5.14c), the 29.11 isopycne is located at lower depth in the northwestern part of the subbasin, because of the steady cyclonic circulation. But it is obvious that in all the Western Mediterranean, the isopycnal surface has been uplifted, compared with the ocean state two years before. This uplift is of the order of about 200 m in the area between the Algerian coast and the Balearic Islands, with higher differences along the Balearic continental slope. The uplift amounts to 400 m in the center of the cyclonic gyre of the Gulf of Lions (from less than 1600 m in October 2004 to less than 1200 m in October 2006). The uplift is the most substantial in the Ligurian subbasin, in which the depth of the 29.11 isopycne varies from 2700 m in October 2004 to about 1800 m in October 2006. This is in good agreement with *Schroeder et al.* (2008), who evidenced an uplift of the $\sigma_{1000} = 33.477$ isopycne of about 100-150 m in the southern part of the subbasin and 200 m in the northern part, up to 1000 m in the Ligurian subbasin.

Figure 5.15 shows the potential density and the horizontal current at 2225 m depth for different days from mid-June to end-December 2005. In June 2005 (Figure 5.15a), $i.e.$ 3 months after the end of the deep convection event, the densest waters have started to exit the former convection area (around 42 °N – 5 °E) and flow southwards along the slope of the Balearic Islands between 42 °N and 40 °N ; the potential density is still high (≥ 29.125 kg.m^{-3}). A cyclone, identified by C1 in Figure 5.15a, starts to trap dense water and to carry it quicker southwards. The separation of the cyclone from the core of the dense water flow seems to be made easier by a northwestwards intrusion of light water, obvious around 41 °N – 5 °E. About one month later in early August 2005 (Figure 5.15b), the cyclone C1 is well defined, around 39 °N – 5.5 °E, with a density gradient higher than 0.01 kg.m^{-3} between the center and the surrounding of the cyclone. It has an horizontal extent of about $1.5° \times 1°$, with an elliptic shape. A second cyclone, identified by C2 in Figure 5.15b, starts to form within the densest part of the water mass (near 40.5 °N – 4.5 °E). At the end of August 2005 (Figure 5.15c), C1 is now located between 38 °N and 39 °N, while C2 starts to move southwards, still along the continental slope of the Balearic Islands. At the end of October 2005 (Figure 5.15d), the signature of C1 is less obvious, while C2 is separating from the flow of the densest water mass. Again, an intrusion of light water occurs simultaneously with the separation of the cyclone C2. In early December 2005 (Figure 5.15e), C2 can be identified at about 39 °N, with an horizontal extent of about $1° \times 1°$ and a more circular shape than C1. A third cyclonic eddy, named C3, starts to appear near 40.5 °N – 4.5 °E. At the end of December 2005 (Figure 5.15f), C3 crosses the 40 °N line and C2 is not identifiable anymore, even if the dense water mass signature which was previously associated with it ($\rho \geq 29.115$ kg.m^{-3}) is still noticeable at 5 °E and between 38 °N and 39 °N. At the end of December 2005, the deep circulation in the Algerian subbasin is more constrained by the cyclonic eastern Algerian gyre (identified by *Testor et al.* (2005b)) than for previous dates.

A vertical subsection through the cyclone C1 at the date of Figure 5.15b (early August 2005) enables to define the vertical signature of this eddy. Figure 5.16a shows the meridian speed and the potential density across C1. A maximum meridian speed of 24 cm.s^{-1} is reached at the surface. It is obvious that C1 is barotropic since it has a vertical extent from the bottom to the surface of the sea. It induces a doming of the isopycnal surfaces, particularly noticeable below the stratified summer surface layer. The layer of water denser than 29.11 kg.m^{-3} is about 1500 m thick in the center of the cyclone, with a weak vertical stratification. Inside C1, below

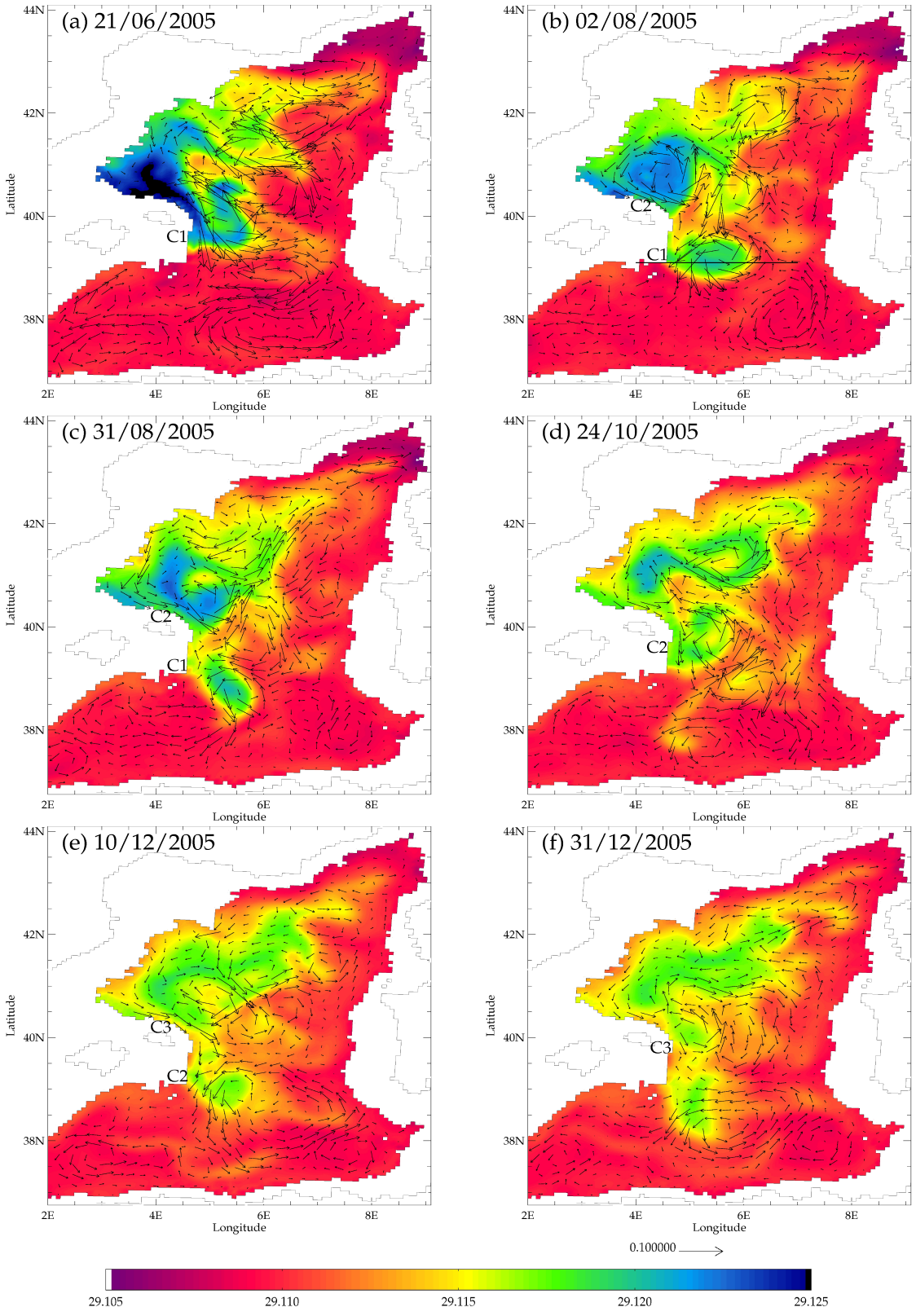

FIG. 5.15 – *Potential density (colors, in kg.m^{-3}) and currents (arrows, in m.s^{-1}), at 2225m depth, in simulation MED12-ARPERA-3, for (a) the 21st June 2005, (b) the 2nd August 2005, (c) the 31st August 2005, (d) the 24th October 2005, (e) the 10th December 2005 and (f) the 31st December 2005. One vector in three is plotted. C1 ,C2 and C3 identify the three successive deep cyclones. The section of Figure 5.16 is drawn on map (b).*

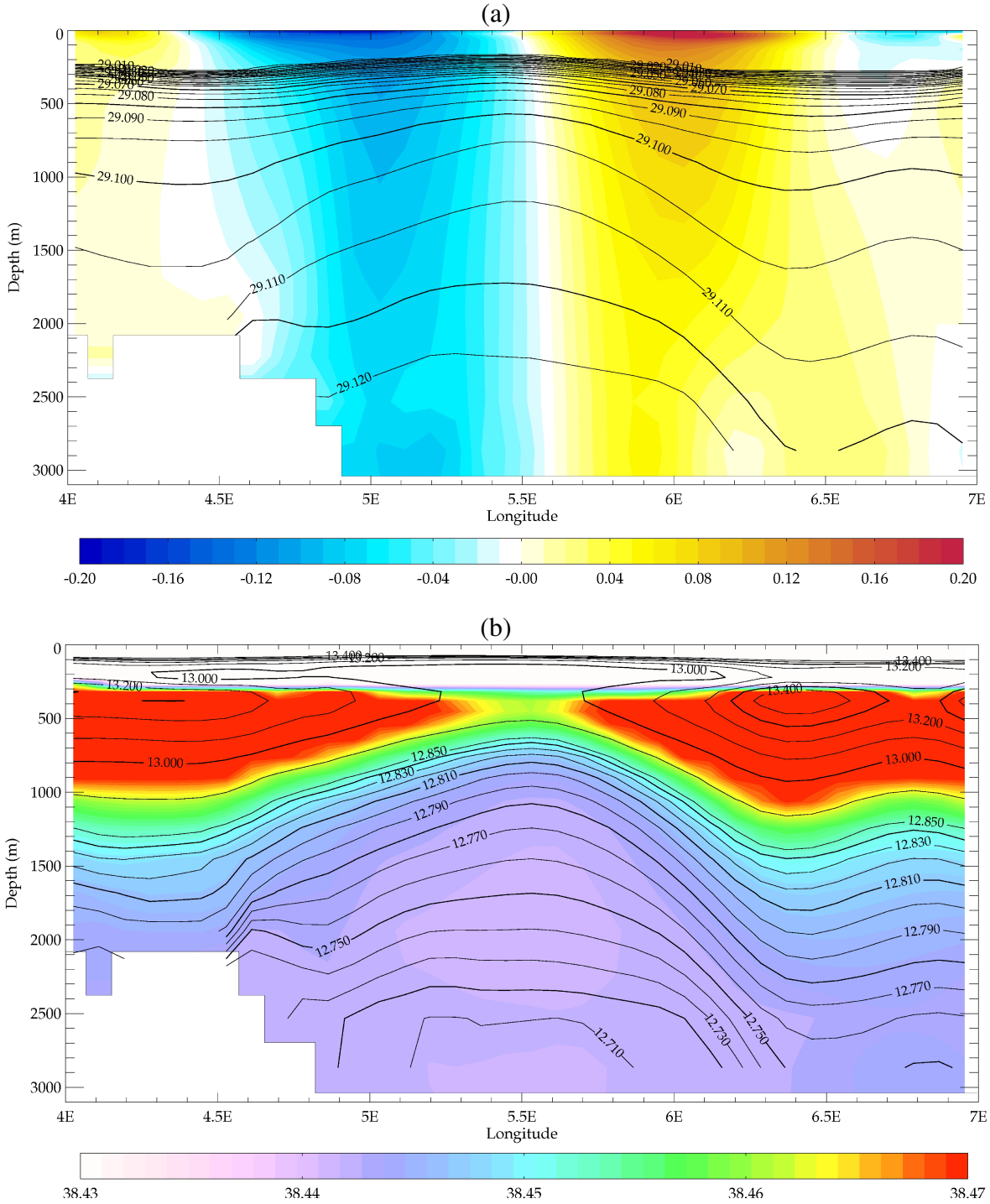

FIG. 5.16 – *Vertical sections at 39.1 °N through cyclone C1, in simulation MED12-ARPERA-3 for the 2nd August 2005. (a) Meridian speed (colors, in m.s^{-1}, negative values for southwards current, positive values for northwards current) and potential density (in kg.m^{-3}, contour lines from 29.00 kg.m^{-3} every 0.005 kg.m^{-3}). (b) Salinity (colors, in psu) and potential temperature (in °C, contour lines every 0.01 °C up to 12.85 °C, then every 0.1 °C from 12.9 °C to 13.5 °C).*

700 m depth, θ ranges between 12.71 and 12.85 °C and S ranges between 38.44 and 38.45 psu (Figure 5.16b). This corresponds well with the values found in the Gulf of Lions during and after the convection event in the simulation. Again, it highlights that the new WMDW in the model is not warm enough and not salty enough compared to in-situ observations made at that time. Around C1, the warm and salty LIW layer is well identifiable, with a core at about 400 m depth ($\theta \geq 13.40$ °C, S ≥ 38.55 psu). The vertical doming induced by C1 is also noticeable for the isothermal and isohaline surfaces (Figure 5.16b).

We have shown with Figure 5.16 that C1 is a barotropic cyclone. So are C2 and C3 (not shown). Thus, their signature in terms of currents can be seen until the sea surface. The Sea Surface Height (SSH) of the model can be used to follow the paths of these cyclonic eddies (Figure 5.17). The comparison between the SSH and the Barotropic Stream Function (BSF, Figure 5.18) allows to distinguish, among the surface eddies identifiable with the SSH, those which are barotropic and which thus carry water throughout the whole water column. Figure 5.18 shows the same dates as Figure 5.15 and 5.17 to easily identify the same cyclones C1, C2 and C3. From June 2005 to December 2005, the cyclonic eddies previously identified have the highest values of BSF in the center of the Algero-Provencal subbasin. About 15 Sv of water over the whole column are carried southwards by C1 in June 2005 (Figure 5.18a), at most 10 Sv are carried southwards by C2 (Figure 5.18b) and at most 7 Sv are carried southwards by C3 (Figure 5.18e). In terms of SSH (Figure 5.17), the three successive barotropic cyclones have a surface signature and move southwards off the coast of Minorca, from 40 °N to 38 °N, between 5 °E and 6 °E. In the model, the southwards propagation of these three successive cyclones lasts more than 6 months, from June 2005 to December 2005.

A comparison with an observed SSH could assess if the eddies identified by the SSH of the model are realistic, and thus if the occurence of deep barotropic cyclones during summer 2005 is credible. Here again, we use the weekly MADTs of AVISO (Figure 5.19). In the observations, two cyclones, CA and CB, propagate successively southwards off the coast of Minorca between early-June 2005 (Figure 5.19a) and early August 2005 (Figure 5.19e). At the end of August 2005, no cyclonic eddy is noticeable in the area of interest (not shown). They are located around 5 °E, whereas in the model C1, C2 and C3 are around 5.5 °E. Nevertheless, the occurence of cyclonic eddies propagating southeastwards then southwards near 40 °N – 5 °E is realistic and confirmed by satellite observations. The time transport of these eddies is estimated at about 2 months. It is about 4 months shorter than in the simulation MED12-ARPERA-3. This slower propagation in the model could be explained by a fewer volume of dense water formed in the model than in reality, which could hinder the spreading of dense water. The vertical resolution of the deep layers in the model could also explain the difficulty of the model to horizontally propagate such dense water mass quickly enough. Finally, *Herrmann et al.* (2008) have shown that the horizontal resolution of the model plays also a role, not only on the spatial scale of the processes that can be resolved by an ocean circulation model, but also on the formation of more energetic eddies. Increasing the horizontal resolution would thus certainly lead to a better representation of the advection time of deep water by barotropic eddies.

Lagrangian view

We adopt here a Lagrangian approach to follow the spreading of the new WMDW formed in winter 2005. We use ARIANE (*Blanke and Raynaud*, 1997), a lagrangian simulator of particles, in an offline configuration with the daily outputs of horizontal and vertical velocities from the simulation MED12-ARPERA-3. In ARIANE, particles are only advected in 3D, they are not affected by mixing or diffusion. We thus start the ARIANE simulation at the end of the deep

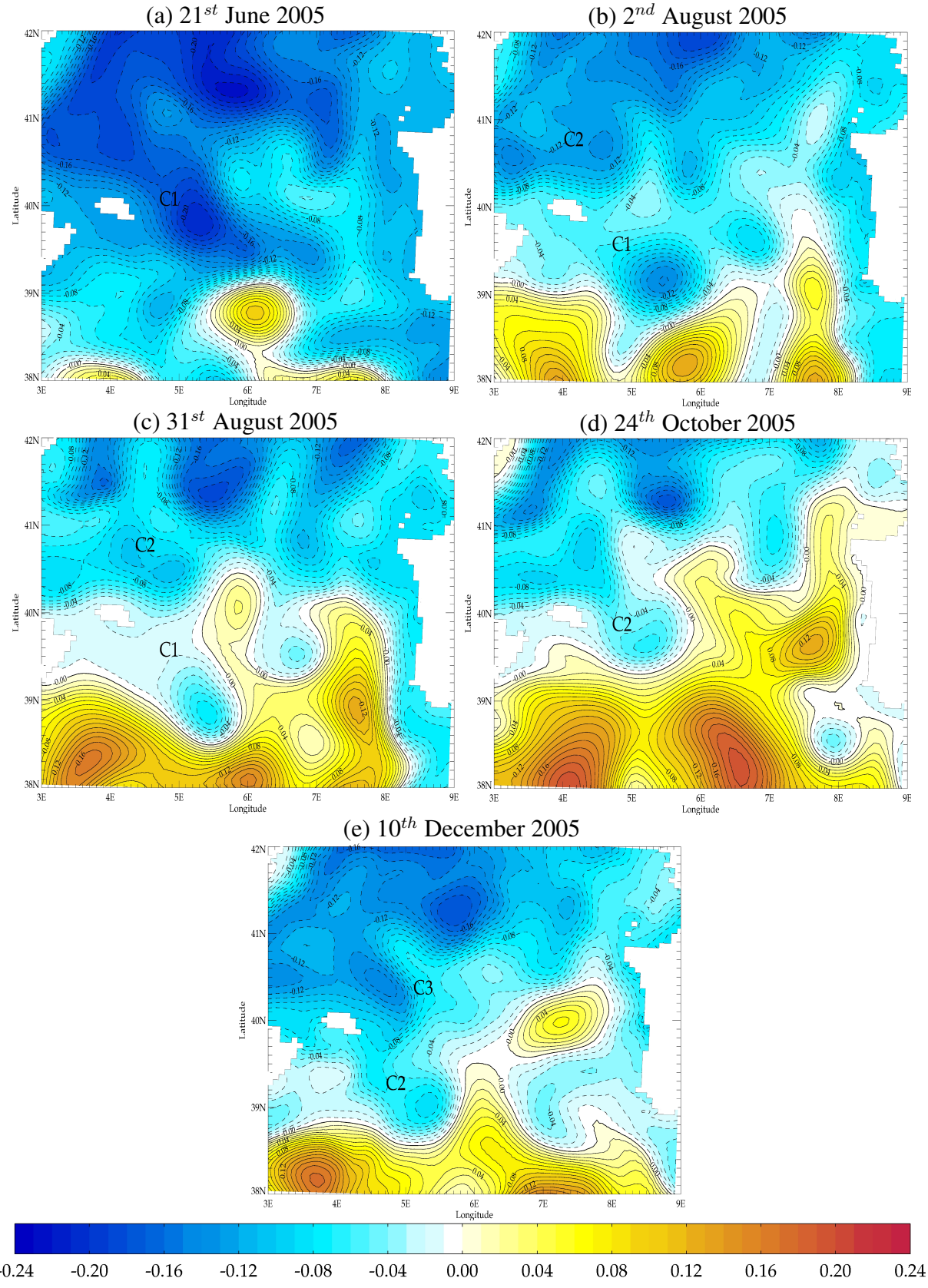

FIG. 5.17 – *Daily averages of the Sea Surface Height (in meters, contours every 0.01 m), in simulation MED12-ARPERA-3, in the center of the Western Mediterranean, for (a) the 21st June 2005, (b) the 2nd August 2005, (c) the 31st August 2005, (d) the 24th October 2005 and (e) the 10th December 2005. C1 ,C2 and C3 identify the three successive deep cyclones.*

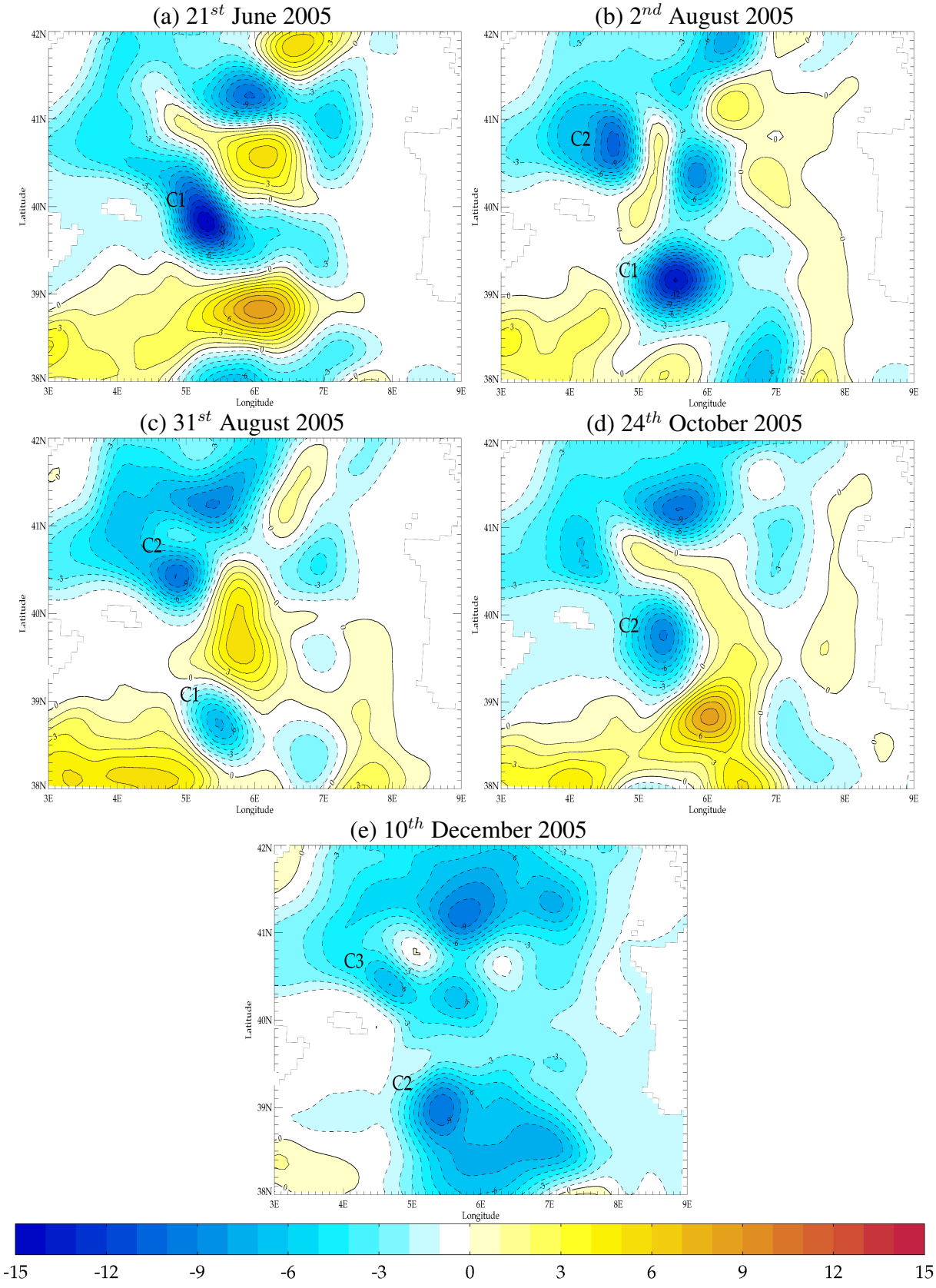

FIG. 5.18 – *Daily averages of the Barotropic Stream Function (in Sv, contours every 1 Sv), in simulation MED12-ARPERA-3, in the center of the Western Mediterranean, for (a) the 21st June 2005, (b) the 2nd August 2005, (c) the 31st August 2005, (d) the 24th October 2005 and (e) the 10th December 2005. C1 ,C2 and C3 identify the three successive deep cyclones.*

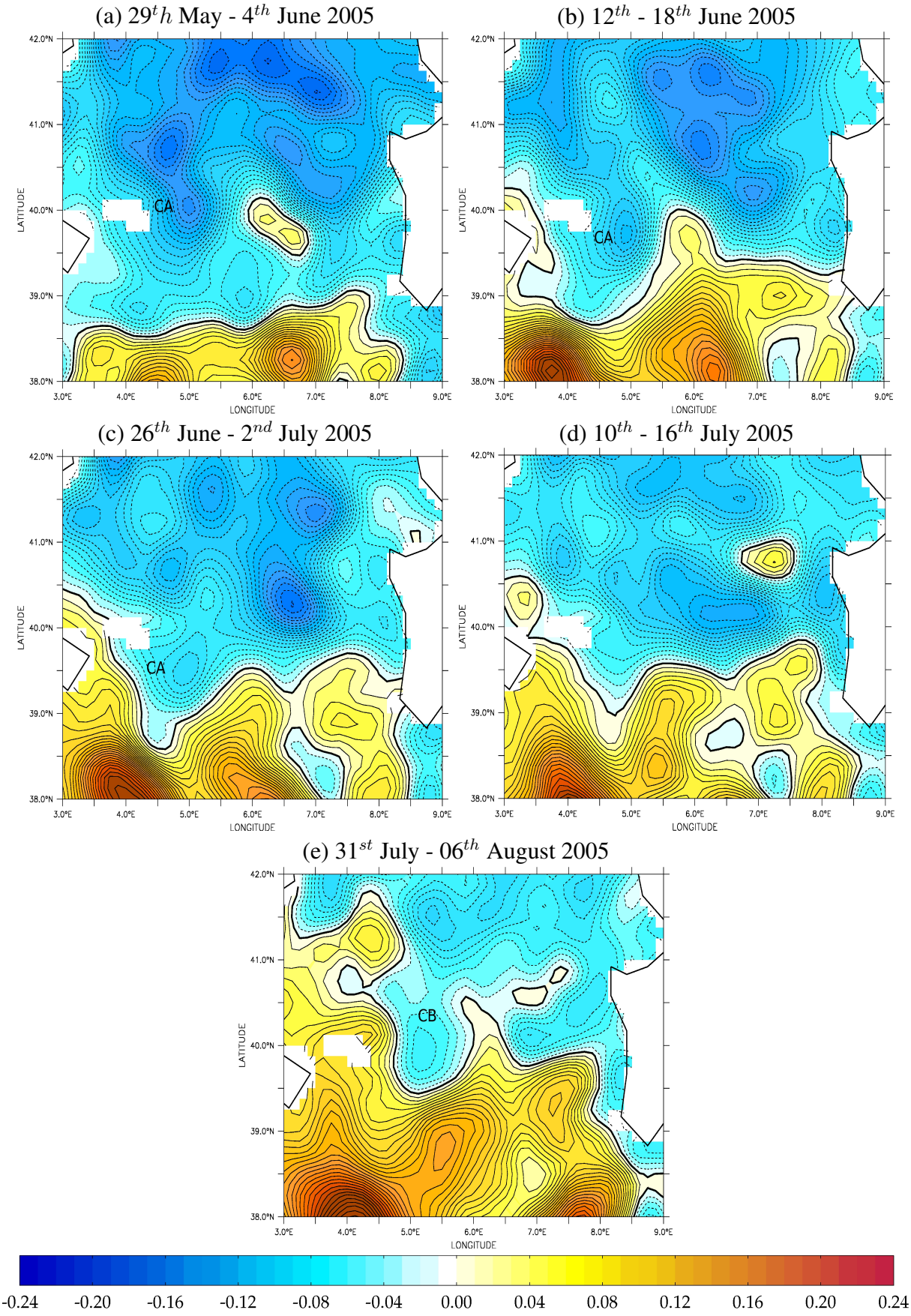

FIG. 5.19 – *Weekly averages of the Sea Surface Height (in meters, contours every 0.01 m), in AVISO observations, in the center of the Western Mediterranean. CA and CB identify two successive cyclones.*